Table 4. Multivariate Analyses of Acute (Grades 2 to 4 and Grades 3 to 4), Chronic, and Extensive-Type Chronic Graft-versus-Host Disease

	Degree of HLA Mismatch	Grade 2-4 acute GVHD				Grade 3-4 acute GVHD			Chronic GVHD				Extensive cGVHD		
		N	RR	(95% CI)	P-value	RR	(95% CI)	P-value	N	RR	(95% CI)	P-value	RR	(95% CI)	P value
Bone marrow transplantation	Single DRB1 (7/8)	248	1.00			1.00			199	1.00			1.00		
	Single A or B (7/8)	137	0.76	(0.55-1.06)	.103	0.91	(0.56-1.47)	.698	111	0.91	(0.61-1.36)	.646	0.89	(0.52-1.50)	.651
	Single C (7/8)	287	0.93	(0.72-1.20)	.584	0.91	(0.61-1.35)	.635	227	1.56	(1.15-2.10)	.004	1.79	(1.22-2.63)	.003
	C + DRB1 (6/8)	144	0.85	(0.60-1.18)	.320	0.88	(0.54-1.44)	.610	109	1.44	(1.01-2.05)	.041	1.47	(0.93-2.32)	.097
	A/B + C (6/8)	122	1.40	(1.04-1.90)	.028	1.90	(1.25-2.87)	.003	87	1.64	(1.14-2.34)	.007	2.26	(1.46-3.50)	<.001
	Other two loci (6/8)	90	0.88	(0.60-1.28)	.501	0.65	(0.34-1.22)	.183	60	1.35	(0.86-2.12)	.191	1.15	(0.62-2.13)	.652
Cord blood transplantation		351	0.55	(0.42-0.72)	<.001	0.43	(0.27-0.58)	<.001	252	1.36	(0.99-1.88)	.057	0.86	(0.55-1.34)	.500

GVHD indicates graft-versus-host disease; cGVHD, chronic graft-versus-host disease.
Adjusted by patient age at transplantation >40 versus <40, patient sex, donor-patient sex mismatch versus matched, ABO major mismatch versus others, advanced versus standard disease status at transplantation, cyclophosphamide, and total-body irradiation or busulfan and cyclophosphamide for conditioning versus other conditioning regimen, and cyclosporine-based versus tacrolimus-based prophylaxis against graft-versus-host disease.

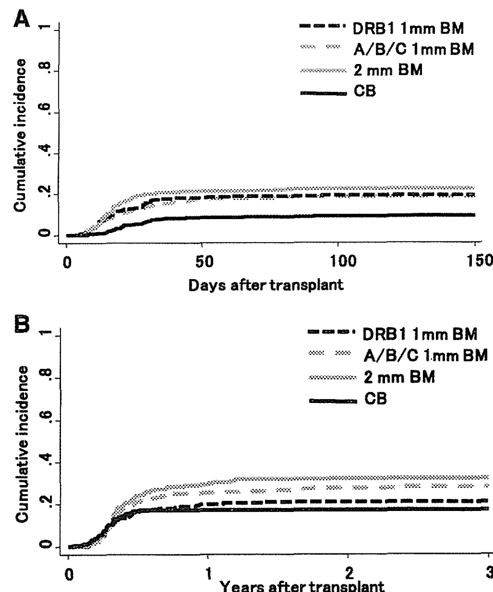

Figure 2. Cumulative incidence of grade 3 to 4 aGVHD (A) and extensive-type cGVHD (B). The cumulative incidences of grade 3 to 4 aGVHD at 100 days posttransplantation for unrelated cord blood recipients, single HLA-DRB1-mismatched unrelated bone marrow (UBM) recipients, and single HLA class I-mismatched UBM were 9%, 19%, 18%, and 22% (A). The cumulative incidences of extensive-type cGVHD at 1-year posttransplantation were 17%, 20%, 25%, and 30% (B).

of UBM recipients included from 1996 and 1999, for which there were no significant outcome differences between UBMT performed in 1996 to 1999 and after 2000. In these periods, there were advances including in supportive care and nutritional management, introduction of new antifungal agents, and more frequent use of tacrolimus, which may have affected transplantation outcomes [27-32].

In conclusion, we suggest that 0 or 2 HLA-mismatched UCB is a comparable second alternative for adult patients with leukemia in the absence of the first alternative, an 8 of 8 UBM donor, with survival similar to that of single DRB1-mismatched or other 7 of 8 UBM recipients. UCB may be preferred over single mismatched UBM when a transplantation is needed urgently, considering the short time needed for UCBT.

ACKNOWLEDGMENTS

The authors are grateful for the assistance and cooperation of all the staff members of the collaborating institutes of the Japan Cord Blood Bank Network and Japan Marrow Donor Program. This work was supported by a Research Grant for Tissue Engineering (H17-014), a Research Grant for Allergic Disease and Immunology (H20-015), a Research Grant for Cancer (H19-1), and a Research Grant for Allergic Disease and Immunology (H23-010) from the Japanese Ministry of Health, Labor, and Welfare.

Financial disclosure: The authors have nothing to disclose.

AUTHORSHIP STATEMENT

Contributions: Y.A., Y.M., R.S., and S. Kato designed the study, and wrote the article; Y.A. analyzed results and created the figures; T.N.I., H.A, and M. Takanashi reviewed and cleaned the Japan Cord Blood Bank Network data, and reviewed the results; S. Taniguchi, S. Takahashi, S. Kai., H.S., Y. Kouzai., N.K., T.M., T.F., and Y. Kodera submitted and cleaned the data; M. Tsuchida, K.K., T.K., and Y.M. reviewed and cleaned the Japan Marrow Donor Program data, and reviewed the results.

SUPPLEMENTARY DATA

Supplementary data related to this article can be found online at doi:10.1016/j.bbmt.2011.10.008.

REFERENCES

1. Morishima Y, Sasazuki T, Inoko H, et al. The clinical significance of human leukocyte antigen (HLA) allele compatibility in patients receiving a marrow transplant from serologically HLA-A, HLA-B, and HLA-DR matched unrelated donors. *Blood.* 2002;99:4200-4206.
2. Morishima Y, Yabe T, Matsuo K, et al. Effects of HLA allele and killer immunoglobulin-like receptor ligand matching on clinical outcome in leukemia patients undergoing transplantation with T-cell-replete marrow from an unrelated donor. *Biol Blood Marrow Transplant.* 2007;13:315-328.
3. Lee SJ, Klein J, Haagenson M, et al. High-resolution donor-recipient HLA matching contributes to the success of unrelated donor marrow transplantation. *Blood.* 2007;110:4576-4583.
4. Bray RA, Hurley CK, Kamani NR, et al. National marrow donor program HLA matching guidelines for unrelated adult donor hematopoietic cell transplants. *Biol Blood Marrow Transplant.* 2008;14:45-53.
5. Sasazuki T, Juji T, Morishima Y, et al. Effect of matching of class I HLA alleles on clinical outcome after transplantation of hematopoietic stem cells from an unrelated donor. Japan Marrow Donor Program. *N Engl J Med.* 1998;339:1177-1185.
6. Gluckman E. Ten years of cord blood transplantation: from bench to bedside. *Br J Haematol.* 2009;147:192-199.
7. Rocha V, Labopin M, Sanz G, et al. Transplants of umbilical-cord blood or bone marrow from unrelated donors in adults with acute leukemia. *N Engl J Med.* 2004;351:2276-2285.
8. Laughlin MJ, Eapen M, Rubinstein P, et al. Outcomes after transplantation of cord blood or bone marrow from unrelated donors in adults with leukemia. *N Engl J Med.* 2004;351:2265-2275.
9. Takahashi S, Iseki T, Ooi J, et al. Single-institute comparative analysis of unrelated bone marrow transplantation and cord blood transplantation for adult patients with hematologic malignancies. *Blood.* 2004;104:3813-3820.
10. Atsuta Y, Suzuki R, Nagamura-Inoue T, et al. Disease-specific analyses of unrelated cord blood transplantation compared with unrelated bone marrow transplantation in adult patients with acute leukemia. *Blood.* 2009;113:1631-1638.
11. Eapen M, Rubinstein P, Zhang MJ, et al. Outcomes of transplantation of unrelated donor umbilical cord blood and bone marrow in children with acute leukaemia: a comparison study. *Lancet.* 2007;369:1947-1954.
12. Eapen M, Rocha V, Sanz G, et al. Effect of graft source on unrelated donor haemopoietic stem-cell transplantation in adults with acute leukaemia: a retrospective analysis. *Lancet Oncol.* 2010;11:653-660.
13. Kodera Y, Morishima Y, Kato S, et al. Analysis of 500 bone marrow transplants from unrelated donors (UR-BMT) facilitated by the Japan Marrow Donor Program: confirmation of UR-BMT as a standard therapy for patients with leukemia and aplastic anemia. *Bone Marrow Transplant.* 1999;24:995-1003.
14. Kawase T, Morishima Y, Matsuo K, et al. High-risk HLA allele mismatch combinations responsible for severe acute graft-versus-host disease and implication for its molecular mechanism. *Blood.* 2007;110:2235-2241.
15. Przepiorka D, Weisdorf D, Martin P, et al. 1994 Consensus conference on acute GVHD grading. *Bone Marrow Transplant.* 1995;15:825-828.
16. Flowers ME, Kansu E, Sullivan KM. Pathophysiology and treatment of graft-versus-host disease. *Hematol Oncol Clin North Am.* 1999;13:1091-1112. viii-ix.
17. Gooley TA, Leisenring W, Crowley J, Storer BE. Estimation of failure probabilities in the presence of competing risks: new representations of old estimators. *Stat Med.* 1999;18:695-706.
18. Gray RJ. A class of k-sample tests for comparing the cumulative incidence of a competing risk. *Ann Stat.* 1988;16:1141-1154.
19. Cox DR. Regression model and life tables. *J R Stat Soc B.* 1972; 34:187-200.
20. Fine JP, Gray RJ. A proportional hazards model for subdistribution of a competing risk. *J Am Stat Assoc.* 1999;94:456-509.
21. Klein JP, Rizzo JD, Zhang MJ, Keiding N. Statistical methods for the analysis and presentation of the results of bone marrow transplants. Part I: unadjusted analysis. *Bone Marrow Transplant.* 2001;28:909-915.
22. Rocha V, Gluckman E. Improving outcomes of cord blood transplantation: HLA matching, cell dose and other graft- and transplantation-related factors. *Br J Haematol.* 2009;147:262-274.
23. Takanashi M, Atsuta Y, Fujiwara K, Kodo H, Kai S, Sato H, et al. The impact of anti-HLA antibodies on unrelated cord blood transplantations. *Blood.* 2010;116:2839-2846.
24. Spellman S, Bray R, Rosen-Bronson S, et al. The detection of donor-directed, HLA-specific alloantibodies in recipients of unrelated hematopoietic cell transplantation is predictive of graft failure. *Blood.* 2010;115:2704-2708.
25. Brunstein CG, Gutman JA, Weisdorf DJ, et al. Allogeneic hematopoietic cell transplantation for hematologic malignancy: relative risks and benefits of double umbilical cord blood. *Blood.* 2010;116:4693-4699.
26. Frassoni F, Gualandi F, Podesta M, et al. Direct intrabone transplant of unrelated cord-blood cells in acute leukaemia: a phase I/II study. *Lancet Oncol.* 2008;9:831-839.
27. Nash RA, Etzioni R, Storb R, et al. Tacrolimus (FK506) alone or in combination with methotrexate or methylprednisolone for the prevention of acute graft-versus-host disease after marrow transplantation from HLA-matched siblings: a single-center study. *Blood.* 1995;85:3746-3753.
28. Yanada M, Emi N, Naoe T, et al. Tacrolimus instead of cyclosporine used for prophylaxis against graft-versus-host disease improves outcome after hematopoietic stem cell transplantation from unrelated donors, but not from HLA-identical sibling donors: a nationwide survey conducted in Japan. *Bone Marrow Transplant.* 2004;34:331-337.
29. Fuji S, Kim SW, Fukuda T, Kamiya S, Kuwahara S, Takaue Y. Positive impact of maintaining minimal caloric intake above 1.0 x basal energy expenditure on the nutritional status of patients undergoing allogeneic hematopoietic stem cell transplantation. *Am J Hematol.* 2009;84:63-64.
30. Fuji S, Kim SW, Mori S, et al. Hyperglycemia during the neutropenic period is associated with a poor outcome in patients undergoing myeloablative allogeneic hematopoietic stem cell transplantation. *Transplantation.* 2007;84:814-820.
31. Upton A, Kirby KA, Carpenter P, Boeckh M, Marr KA. Invasive aspergillosis following hematopoietic cell transplantation: outcomes and prognostic factors associated with mortality. *Clin Infect Dis.* 2007;44:531-540.
32. Yokoe D, Casper C, Dubberke E, et al. Infection prevention and control in health-care facilities in which hematopoietic cell transplant recipients are treated. *Bone Marrow Transplant.* 2009;44: 495-507.

Int J Hematol (2012) 96:485–491
DOI 10.1007/s12185-012-1165-z

ORIGINAL ARTICLE

Phase 1 trial of gemtuzumab ozogamicin in combination with enocitabine and daunorubicin for elderly patients with relapsed or refractory acute myeloid leukemia: Japan Adult Leukemia Study Group (JALSG)-GML208 study

Yoshikazu Ito · Atsushi Wakita · Satoru Takada · Masahiro Mihara · Moritaka Gotoh · Kazuma Ohyashiki · Shigeki Ohtake · Shuichi Miyawaki · Kazunori Ohnishi · Tomoki Naoe

Received: 20 June 2012 / Revised: 17 August 2012 / Accepted: 20 August 2012 / Published online: 6 September 2012
© The Japanese Society of Hematology 2012

Abstract We conducted a phase 1 study of a combination of gemtuzumab ozogamicin (GO) plus conventional chemotherapy in elderly patients (≥65 years old) with relapsed or refractory CD33-positive acute myeloid leukemia (AML). Patients received a standard dose of enocitabine (200 mg/m^2 × 8 days) and daunorubicin (30 mg/m^2 × days 1–3) plus an escalating dose of GO (1.5–5 mg/m^2 on day 4). The dose escalation of GO was done according to a standard 3 + 3 design following a modified Fibonacci sequence. No dose-limiting toxicities were observed in three patients (median age, 71) at level 1 (1.5 mg/m^2) or in three patients (median age, 73) at level 2 (3 mg/m^2). Neither veno-occlusive diseases nor sinusoidal obstructive syndromes were noted at either level. However, as GO was withdrawn from the US market in June 2010, based on a randomized study in newly diagnosed AML, we decided not to proceed to the level 3 (5 mg/m^2) in order to avoid possibly more severe adverse effects, and also because all six patients experienced grade 4 myelosuppression, with complete remission in three. This study showed that 3 mg/m^2 of GO in combination with enocitabine and daunorubicin may be a recommendable dose for a phase 2 study in Japanese elderly patients with CD33-positive AML. The study was registered at the University Hospital Medical Information Network (UMIN) Clinical Trials Registry (http://www.umin.ac.jp/ctr/) as UMIN000002603.

Keywords Acute myeloid leukemia · Elderly · Gemtuzumab ozogamicin · Chemotherapy

Introduction

Therapeutic strategy for acute myeloid leukemia (AML) generally consists of two phases: intensive combination chemotherapy to achieve complete remission (CR) followed by post-remission therapy to prevent relapse with 3–4 courses of intensive combination chemotherapy or with hematopoietic stem cell transplantation (HSCT). Recently, with these intensive treatments, nearly 80 % of

Y. Ito (✉) · M. Gotoh · K. Ohyashiki
Division of Hematology, First Department of Internal Medicine, Tokyo Medical University, 6-7-1 Nishishinjuku, Shinjuku-ku, Tokyo 160-0023, Japan
e-mail: yito@tokyo-med.ac.jp

A. Wakita
Department of Hematology and Oncology, Nagoya City West Medical Center, Nagoya, Japan

S. Takada
Leukemia Research Center, Saiseikai Maebashi Hospital, Maebashi, Japan

M. Mihara
Division of Hematology, Fujioka General Hospital, Fujioka, Japan

S. Ohtake
Department of Clinical Laboratory Science, Kanazawa University Graduate School of Medical Science, Kanazawa, Japan

S. Miyawaki
Hematology Division, Tokyo Metropolitan Ohtsuka Hospital, Tokyo, Japan

K. Ohnishi
Department of Internal Medicine 3, Oncology Center, Hamamatsu University School of Medicine, Hamamatsu, Japan

T. Naoe
Department of Hematology and Oncology, Nagoya University Graduate School of Medicine, Nagoya, Japan

younger AML patients less than 60 or 65 years obtain CR and nearly 50 % enjoy long-term survival [1].

However, it is not the case with elderly AML patients, as less than 60 % of them achieve CR and less than 20 % secure long-term survival, partly because AML of elderly patients carries biologically unfavorable characteristics compared with those of younger patients, and partly because elderly patients cannot tolerate intensive therapies including HSCT [1–3]. Therefore, collective efforts have been made in the past decades to improve the prognosis of elderly AML patients by employing new drugs and strategies, without any remarkable progress [1, 2].

Gemtuzumab ozogamicin (GO) is a recombinant humanized anti-CD33 monoclonal antibody, conjugated to calicheamicin which is around 1000 times more potent than doxorubicin [4, 5], and a promising novel agent against AML. Since CD33 antigen is expressed on around 90 % of AML cells, GO is attached to the antigen on cell surface and rapidly internalized. Then, the linker of calicheamicin and CD33 is hydrolyzed, and isolated calicheamicin causes subsequent cell death in CD33-positive cells. GO was shown to be effective in patients with relapsed AML and was approved for relapsed elderly AML in the United States [6, 7], and also for relapsed/refractory AML in Japan in 2005 [8].

Since monotherapy with GO alone has resulted in limited efficacy in relapsed AML, combination of GO with conventional anti-leukemia drugs has been tested by several investigators, and resulted in favorable but some conflicting outcomes [9–11]. We conducted a phase 1 study of combination therapy of GO with enocitabine [behenoyl-arabinofuranosyl-cytosine (BHAC)] and daunorubicin (DNR) in elderly patients with relapsed/refractory AML, because there had been no phase 1 study to find the optimal dosage of GO in combination with conventional chemotherapy for elderly AML including Japan where only monotherapy was approved by its national medical insurance. Instead of cytarabine (Ara-C), its analog, BHAC, was chosen for this study. BHAC is resistant to deamination by cytidine deaminase because of enhanced lipophilicity by behenoylation at the 4-amino position of the cytosine, and is converted to cytarabine within and without leukemic cells. BHAC had been widely used for elderly AML patients in Japan owing to its easier administration method by 3-h infusion, compared with 24-h continuous infusion of Ara-C and less adverse events compared with Ara-C [12, 13].

Patients and methods

Patients

Three JALSG member institutions participated in this prospective study. The inclusion criteria of patients were as follows: (a) diagnosed as CD33-positive AML (excluding acute promyelocytic leukemia). The positivity was defined when 20 % or more blasts were positive for CD33 by flow-cytometry; (b) relapsed after the first CR (CR1) or were refractory to initial standard induction therapy; (c) 65–74 years old; (d) 0–1 by Eastern Cooperative Oncology Group (ECOG) performance status; (e) no active double cancer; (f) adequate cardiac, renal and hepatic function; (g) no uncontrolled infection; (h) no HIV, HBV and HCV infection. Cytogenetic abnormalities were grouped by standard criteria and classified according to the UK Medical Research Council (MRC) classification [14]. All patients were hospitalized during the therapy and received the best supportive care if needed.

Study design and treatment protocol

The primary objective of this study was to determine the maximum tolerable dose (MTD) from the dose-limiting toxicity (DLT) of GO in combination with standard doses of BHAC and DNR in elderly Japanese AML patients. All unknown ≥grade 3 and already known ≥grade 4 non-hematological toxicities, and persistent ≥grade 4 neutropenia, lymphopenia or anemia by the Common Terminology Criteria for Adverse Events (CTCAE) version 3.0 that occurred, unrelated to leukemia progression until 30 days after the treatment, were considered DLTs. Secondary objective was to evaluate the remission rate and other toxicities of the combination therapy.

Remission induction consisted of BHAC 200 mg/m^2 by 3-h intravenous infusion for 8 days, DNR 30 mg/m^2 by 30-min intravenous infusion for 3 days from day 1, and escalating dose of GO (provided by the Nonprofit Supportive Organization for Cooperative Study on Adult Leukemia Treatment, which purchased it from Weiss Co. Ltd, Japan, and distributed to each participating institution): 1.5 mg/m^2 (level 1), 3 mg/m^2 (level 2) and 5 mg/m^2 (level 3) by 2-h intravenous infusion on day 4. The dose of GO was escalated according to the standard 3 + 3 design (Fig. 1). To prevent the infusion reaction of GO, antihistamines and corticosteroids were given 1 h before the infusion.

The study was approved by the Institutional Review Board at each participating hospitals. Written informed consent was obtained from each patient before registration in accordance with the Declaration of Helsinki. The study was registered at the University Hospital Medical Information Network (UMIN) Clinical Trials Registry (http://www.umin.ac.jp/ctr/) as UMIN000002603.

Response criteria

Responses were evaluated according to the recommendations of the International Working Group [15]. A CR was

defined as disappearance of all clinical and/or radiologic evidence of the disease with ≤5 % marrow blasts, neutrophil count ≥1 × 10^9/L, and platelet count ≥100 × 10^9/L.

Results

The study was initiated in December 2008, and 3 patients were enrolled to the level 1. Median age of patients was 73 and all were refractory to initial induction therapy (Table 1). None experienced DLT although all had grade 4 neutropenia and thrombocytopenia and grade 3 febrile neutropenia (Table 2). Grade 1/2 non-hematological toxicities included hypoalbuminemia and hyperglycemia in 3, hyponatremia in 2, hyperbilirubinemia and hypokalemia in one. Then another 3 patients were enrolled to the level 2, with median age of 71 with one relapsed case and 2 refractory. Again none experienced DLT, although all had grade 4 neutropenia and thrombocytopenia and 2 had grade 3 febrile neutropenia. Grade 1/2 non-hematological toxicities included hypoalbuminemia and diarrhea in 3, hyperglycemia, hyponatremia and elevated aminotransferases in 2, hyperbilirubinemia, elevated creatinine and pruritis in one. In June 2010, however, GO was withdrawn from the US market based on the result of a randomized study in newly diagnosed younger AML patients conducted by the South Western Oncology Group (SWOG), which resulted in the lack of improvement in CR rate or relapse-free survival (RFS) and in the higher fatal induction adverse-event rate in the GO arm [11]. Therefore, by the recommendation of the independent data and safety monitoring committee, we decided not to proceed to the level 3 (5 mg/m^2) in order to avoid plausible higher adverse events to patients and partly because all 6 patients in the levels 1 and 2 experienced grade 4 myelosuppression.

In all 6 patients, sufficient hypoplasia of bone marrow was obtained on day 15. Two patients at the level 1 and one at the level 2 obtained CR, of whom both at the level 1 were refractory cases. Karyotypes of these two cases were 46,XY,i(14)(q10) (9/20 cells) and 47,XX, +8 (10/23 cells), respectively. Another CR case after relapse at the level 2 showed a normal female karyotype. One patient at the level 2 died at 5 months due to disease progression, but other 5 were alive at least for 6 months after the initiation of this treatment.

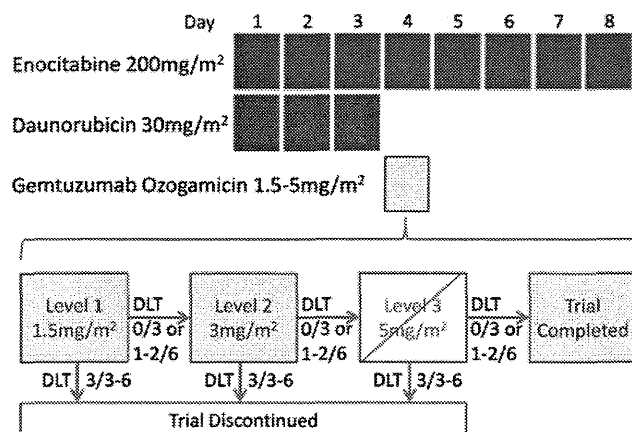

Fig. 1 Treatment schedule. Gemtuzumab ozogamicin (GO) was scheduled to be escalated from 1.5 to 3 and 5 mg/m^2

Table 1 Patient characteristics and outcome of treatment

Age	65, 73, 74	69, 71, 74
Male/female	1/2	2/1
WBC, $\times 10^9$/L	1.1, 3.4, 3.5	2.0, 3.5, 6.1
Blasts (%)	13.9, 18.9, 61.0	29.2, 41.9, 55.8
CD33 positivity (%)	45.8, 84.6, 99.1	82.2, 94.0, 99.3
Relapsed/refractory	0/3	1/2
Months after onset	1, 1, 1	1, 3, 14
Cytogenetics		
Intermediate	3	1
Adverse	0	2
Performance status		
0	3	1
1	0	2
Outcome of treatment		
Hypoplastic marrow on day 15	3	3
CR	2	1
Alive on day 38	3	3
Alive after 6 months	3	2

The number of patients is given in each column
WBC white blood cells

Discussion

Although GO, a CD33-targeting humanized antibody conjugated with calicheamicin, is a promising agent for AML by its unique mode of action, the efficacy of its monotherapy is limited, resulting in 25–30 % CR in relapsed AML patients in USA and Europe as well as in Japan [6–8]. Therefore, the role of GO in combination with conventional anti-leukemia drugs has been explored by several investigators [16]. In Japan, JALSG previously conducted a phase 1 study of GO in combination with standard induction chemotherapy in relapsed/refractory younger AML patients, and reported that 5 mg/m^2 of GO caused DLTs in 3 of 3 patients and the recommendable dose of GO for a phase 2 study was 3 mg/m^2 in combination with standard doses of DNR or idarubicin (IDR) and Ara-C in younger AML patients [17].

In the present phase 1 study for elderly AML patients, no DLT was observed up to 3 mg/m^2 GO in combination

with BHAC and DNR, but we did not enroll patients for the scheduled 5 mg/m^2 according to the recommendation of the independent data and safety monitoring committee, mainly because fatal toxicity profiles had occurred in the SWOG S0106 study by using 6 mg/m^2 of GO [11] and in the JALSG AML206 study 5 mg/m^2 of GO [17].

Although this study for elderly patients was different from our previous study in younger patients, we used the standard drug combination and dosage for both younger and elderly AML. Therefore, our decision to regard 3 mg/m^2 as the recommendable dose for a phase 2 study, without enrolling patients further to the level 3 or 5 mg/m^2 of GO, would be justified.

Combination therapy of GO with conventional chemotherapy for elderly AML patients has already been tested by other investigators as summarized in Table 3 [10, 18–25]. Although the stage of leukemia and the dosage of GO, as well as combined anti-leukemia drugs and their dosage, are different, the combination therapies have generated satisfactory CR rates (35–81 %) in elderly patients of age 50–83 years. Two Italian groups employed 3 mg/m^2 of GO in combination with chemotherapy, showing its feasibility in elderly patients [22, 23]. Therefore, we decided to initiate our phase 1 study with the half dose of GO (1.5 mg/m^2), considering the possible ethnic difference between Europeans and Japanese. Notably among these reports was the Korean group that conducted a phase 2 study in 37 newly diagnosed elderly AML patients of age $\geq$55 by 6 mg/m^2 of GO on day 1 combined with BHAC 300 mg/m^2 for 5 days and IDR 12 mg/m^2 for 3 days, and reported CR in 28 patients (78 %), CR with incomplete platelet recovery (CRp) in 2 (3 %), induction death in 2, grade 4 adverse events in 2, and 25 patients (68 %) living at the time of report [24]. Although this was not a randomized study, their high CR/CRp rate in elderly AML patients is quite satisfactory.

As mentioned above, but reported only as an abstract so far, SWOG conducted a randomized study comparing DNR 60 mg/m^2 for 3 days and Ara-C 100 mg/m^2 for 7 days versus DNR 45 mg/m^2 for 3 days and Ara-C 100 mg/m^2 for 7 days plus GO 6 mg/m^2 on day 4 in 627 newly diagnosed younger AML patients of age 18–60 [11]. There were no differences in CR rates (66 vs. 69 %) nor in RFS, but the rate of fatal adverse events possibly attributable to treatment was significantly higher in the GO arm (5.8 vs. 0.8 %, $P = 0.002$). It should be argued that the doses of DNR were not the same in the above two groups, and their CR rates are substantially lower even in the DNR + Ara-C arm as compared with those of other cooperative study groups including JALSG, which reported nearly 80 % CR in younger AML patients of age 15–64 years [26]. Nevertheless, GO has been withdrawn from the US market based on the SWOG study.

On the contrary, however, the United Kingdom Medical Research Council reported that a substantial proportion of younger patients with AML had improved survival with the addition of GO to induction chemotherapy with little additional toxicity [9]. They conducted a randomized study comparing GO 3 mg/m^2 on day 1 combined with DNR and Ara-C or with DNR, Ara-C and etoposide in 1113 patients, predominantly younger than age 60. The addition of GO was well tolerated with no significant increase in toxicity, with no overall difference in CR (82 vs. 83 %) or survival. However, a predefined analysis by cytogenetics showed highly significant interaction with GO in induction therapy ($P = 0.001$); significant survival benefit for patients with favorable cytogenetics, no benefit for patients with poor-risk disease, and a trend for benefit in intermediate-risk patients. An internally validated prognostic index identified that approximately 70 % of patients had a predicted benefit of 10 % by GO in 5-year survival.

Thus, the efficacy and role of GO in combination with conventional chemotherapy have not been determined even

Table 2 Hematological toxicities

	Neutrophils			Platelets		
Registration number in each cohort:	1	2	3	1	2	3
Level 1						
Days to nadir	17	18	15	14	14	15
Count at nadir, $\times 10^9$/L	0.016	0	0.009	18	5	15
CTCAE grade	4	4	4	4	4	4
Days to recover to grade 2	36	30	22	22	30	25
Level 2						
Days to nadir	15	15	18	15	13	9
Count at nadir, $\times 10^9$/L	0.067	0.038	0	16	13	15
CTCAE grade	4	4	4	4	4	4
Days to recover to grade 2	22	27	35	29	No	27

Table 3 GO combined chemotherapy for elderly patients with AML

References	Phase	Age	Status of AML	Combined agents	Dose (mg/m^2)	Days treated	Dose of GO (mg/m^2)	Schedule of GO	No. of pts	Grade 5 (*n*)	VOD (*n*)	CR or CRp (%)	Median OS (m)
De Angelo [18] (abstr)	2	62–78	New	Ara-C	100	7	6, 6	d1, d8	21	0	0	48	13. 4
Piccaluga [19]	Not mentioned	50–71	New/Rel/Ref	Ara-C	100	7	6, 4	d1, d8	9	1	0	56	6
Brunnberg [25]	2	60–83	New	Ara-C	100	7	6, 4	d1, d8	57	11	5	58	10
Stone [20]	1/2	52–69	Rel/Ref	Ara-C	3000	5	9	d7	37	7	0	35	8.9
Stone [20]	1/2	52–69	Rel/Ref	Ara-C	3000	5	9, 4. 5	d7, d14	7	4	0	Not reported	Not reported
Fianchi [21]	Not mentioned	65–78	New/Rel/Ref	Ara-C	100	5–7	6	d9	53	7	1	45	9
				G-CSF	5 μg/kg	8							
Clavio [22]	Not mentioned	60–80	New	Ara-C	1000	3	3	d4	46	1	0	52	8
				IDR	5	3							
				Fludarabine	30	3							
Pirrotta [23]	Not mentioned	65–77	New	Ara-C	1000 × 2	3	3	d4	10	0	0	60	10.5
				IDR	5	3							
				Fludarabine	25 × 2	3							
Eom [24]	Not mentioned	55–76	New	BHAC	300	5	6	d1	37	2	2	78.4	Not reported
				IDR	12	3							
Castaigne [10]	3	50–70	New	Ara-C	200	7	3, 3, 3	d1, d4, d7	139	9	3	81	34
				DNR	60	3							

New newly diagnosed, *Rel* relapsed, *Ref* refractory, *Ara-C* cytarabine, *BHAC* enocitabine, *IDR* idarubicin, *DNR* daunorubicin, *VOD* veno-occlusive disease, *CR* complete remission, *CRp* CR with incomplete platelet recovery

in AML of younger patients yet. The present study demonstrates that 3 mg/m^2 of GO with conventional BHAC + DNR can be administered safely in elderly patients with relapsed/refractory AML. Further study with this combination regimen will be warranted for elderly AML, for which the standard therapy has not been established so far, as either initial or salvage therapy.

Acknowledgments This work was supported in part by grants from the Ministry of Health, Labour and Welfare, Health Labour Sciences Research Grant on Clinical Cancer Research 004, National Cancer Center Research and Development Fund 23-A-23 and the Nonprofit Supportive Organization for Cooperative Study on Adult Leukemia Treatment. We thank Dr. Ryuzo Ohno for his advice and assistance during the entire study as well as the preparation of manuscript, and Drs. Seiji Kojima, Atsushi Manabe and Shigesaburo Miyakoshi of the Data and Safety Monitoring Committee for their review.

Conflict of interest The authors have no conflict of interest.

References

1. Burnett A, Wetzler M, Lowenberg B. Therapeutic advances in acute myeloid leukemia. J Clin Oncol. 2011;29:487–94.
2. Dombret H, Raffoux E, Gardin C. Acute myeloid leukemia in the elderly. Semin Oncol. 2008;35:430–8.
3. Buchner T, Berdel WE, Wormann B, Schoch C, Haferlach T, Schnittger S, et al. Treatment of older patients with AML. Crit Rev Oncol Hematol. 2005;56:247–59.
4. Sievers EL, Larson RA, Stadtmauer EA, Estey E, Lowenberg B, Dombret H, et al. Efficacy and safety of gemtuzumab ozogamicin in patients with CD33-positive acute myeloid leukemia in first relapse. J Clin Oncol. 2001;19:3244–54.
5. Larson RA. Current use and future development of gemtuzumab ozogamicin. Semin Hematol. 2001;38(suppl 6):24–31.
6. Bross PF, Beitz J, Chen G, Chen XH, Duffy E, Kieffer L, et al. Approval summary: gemtuzumab ozogamicin in relapsed acute myeloid leukemia. Clin Cancer Res. 2001;7:1490–6.
7. Larson RA, Boogaerts M, Estey E, Karanes C, Stadtmauer EA, Sievers EL, et al. Antibody-targeted chemotherapy of older patients with acute myeloid leukemia in first relapse using Mylotarg (gemtuzumab ozogamicin). Leukemia. 2002;16:1627–36.
8. Kobayashi Y, Tobinai K, Takeshita A, Naito K, Asai O, Dobashi N, et al. Phase I/II study of humanized anti-CD33 antibody conjugated with calicheamicin, gemtuzumab ozogamicin, in relapsed or refractory acute myeloid leukemia: final results of Japanese multicenter cooperative study. Int J Hematol. 2009;89: 460–9.
9. Burnett AK, Hills RK, Milligan D, Kjeldsen L, Kell J, Russell NH, et al. Identification of patients with acute myeloblastic leukemia who benefit from the addition of gemtuzumab ozogamicin: results of the MRC AML15 trial. J Clin Oncol. 2011;29:369–77.
10. Castaigne S, Pautas C, Terré C, Raffoux E, Bordessoule D, Bastie JN, et al. Effect of gemtuzumab ozogamicin on survival of adult patients with de novo acute myeloid leukaemia (ALFA-0701): a randomised, open-label, phase 3 study. Lancet. 2012;379: 1508–16.
11. Petersdorf S, Kopecky K, Stuart RK, Larson RA, Nevill TJ, Stenke L, et al. Preliminary results of Southwest Oncology Group Study S0106: an international intergroup phase 3 randomized trial comparing the addition of gemtuzumab ozogamicin to standard induction therapy versus standard induction therapy followed by a second randomization to post-consolidation gemtuzumab ozogamicin versus no additional therapy for previously untreated acute myeloid leukemia. Blood. 2009;114:326–7a (Abstract 790).
12. Mori M, Ohta M, Miyata A, Higashihara M, Oshimi K, Kimura H, et al. Treatment of acute myeloid leukemia patients aged more than 75 years: results of the E-AML-01 trial of the Japanese Elderly Leukemia and Lymphoma Study Group (JELLSG). Leuk Lymphoma. 2006;47:2062–9.
13. Wakita A, Ohtake S, Takada S, Yagasaki F, Komatsu H, Miyazaki Y, et al. Randomized comparison of fixed-schedule versus response-oriented individualized induction therapy and use of ubenimex during and after consolidation therapy for elderly patients with acute myeloid leukemia: the JALSG GML200 Study. Int J Hematol. 2012;96:84–93.
14. Grimwade D, Walker H, Oliver F, Wheatley K, Harrison C, Harrison G, et al. The importance of diagnostic cytogenetics on outcome in AML: analysis of 1,612 patients entered into the MRC AML 10 trial. Blood. 1998;92:2322–33.
15. Cheson BD, Bennett JM, Kopecky KJ, Buchner T, Willman CL, Estey EH, et al. Revised recommendations of the international working group for diagnosis, standardization of response criteria, treatment outcomes, and reporting standards for therapeutic trials in acute myeloid leukemia. J Clin Oncol. 2003;21:4642–9.
16. Tanaka M, Kano Y, Akutsu M, Tsunoda S, Izumi T, Yazawa Y, et al. The cytotoxic effects of gemtuzumab ozogamicin (Mylotarg) in combination with conventional antileukemic agents by isobologram analysis in vitro. Anticancer Res. 2009;29:4589–96.
17. Usui N, Takeshita A, Nakaseko C, Dobashi N, Fujita H, Kiyoi H, et al. Phase I trial of gemtuzumab ozogamicin in intensive combination chemotherapy for relapsed or refractory adult acute myeloid leukemia (AML): Japan Adult Leukemia Study Group (JALSG)-AML206 study. Cancer Sci. 2011;102:1358–65.
18. De Angelo DJ, Stone RM, Durrant S, Liu DL, Baccarani M, Schiffer CA, et al. Gemtuzumab ozogamicin (Mylotarg (R)) in combination with induction chemotherapy for the treatment of patients with de novo acute myeloid leukemia: Two age-specific phase 2 trials. Blood. 2003;102:100a (Abstract 341).
19. Piccaluga PP, Martinelli G, Rondoni M, Malagola M, Gaitani S, Visani G, et al. First experience with gemtuzumab ozogamicin plus cytarabine as continuous infusion for elderly acute myeloid leukaemia patients. Leuk Res. 2004;28:987–90.
20. Stone RM, Moser B, Sanford B, Schulman P, Kolitz JE, Allen S, et al. High dose cytarabine plus gemtuzumab ozogamicin for patients with relapsed or refractory acute myeloid leukemia: cancer and Leukemia Group B study 19902. Leuk Res. 2011;35:329–33.
21. Fianchi L, Pagano L, Leoni F, Storti S, Voso MT, Valentini CG, et al. Gemtuzumab ozogamicin, cytosine arabinoside, G-CSF combination (G-AraMy) in the treatment of elderly patients with poor-prognosis acute myeloid leukemia. Ann Oncol. 2008;19: 128–34.
22. Clavio M, Vignolo L, Albarello A, Varaldo R, Pierri I, Catania G, et al. Adding low-dose gemtuzumab ozogamicin to fludarabine, Ara-C and idarubicin (MY-FLAI) may improve disease-free and overall survival in elderly patients with non-M3 acute myeloid leukaemia: results of a prospective, pilot, multi-centre trial and comparison with a historical cohort of patients. Br J Haematol. 2007;138:186–95.
23. Pirrotta MT, Bocchia M, Bucalossi A, Defina M, Forconi F, Gozzetti A, et al. Pilot study of gemtuzumab ozogamicin (GO), fludarabine, cytarabine and idarubicin combined regimen (GO-FLAI) as first-line induction therapy plus GO alone as consolidation therapy for elderly acute myeloid leukemia patients. Acta Haematol. 2007;118:7–9.
24. Eom KS, Kim HJ, Min WS, Lee S, Min CK, Cho BS, et al. Gemtuzumab ozogamicin in combination with attenuated doses

of standard induction chemotherapy can successfully induce complete remission without increasing toxicity in patients with acute myeloid leukemia aged 55 or older. Eur J Haematol. 2007;79:398–404.
25. Brunnberg U, Mohr M, Noppeney R, Dürk HA, Sauerland MC, Müller-Tidow C, et al. Induction therapy of AML with ara-C plus daunorubicin versus ara-C plus gemtuzumab ozogamicin: a randomized phase II trial in elderly patients. Ann Oncol. 2012;23:990–6.
26. Ohtake S, Miyawaki S, Fujita H, Kiyoi H, Shinagawa K, Usui N, et al. Randomized study of induction therapy comparing standard-dose idarubicin with high-dose daunorubicin in adult patients with previously untreated acute myeloid leukemia: the JALSG AML201 Study. Blood. 2011;117:2358–65.

Springer

OPEN ACCESS Freely available online PLoS one

The Clathrin Assembly Protein PICALM Is Required for Erythroid Maturation and Transferrin Internalization in Mice

Mai Suzuki[1], Hirokazu Tanaka[2], Akira Tanimura[3], Kenji Tanabe[4], Natsuko Oe[4], Shinya Rai[2], Syunsuke Kon[5], Manabu Fukumoto[6], Kohji Takei[4], Takaya Abe[7], Itaru Matsumura[2], Yuzuru Kanakura[3], Toshio Watanabe[1]*

1 Department of Biological Science, Graduate School of Humanities and Sciences, Nara Women's University, Nara, Japan, **2** Division of Hematology, Department of Internal Medicine, Kinki University, Osaka, Japan, **3** Department of Hematology and Oncology, Osaka University Graduate School of Medicine, Osaka, Japan, **4** Department of Neuroscience, Okayama University Graduate School of Medicine, Dentistry, and Pharmaceutical Sciences, Okayama, Japan, **5** Department of Molecular Immunology, Institute of Development, Aging and Cancer, Tohoku University, Sendai, Japan, **6** Department of Pathology, Institute of Development, Aging and Cancer, Tohoku University, Sendai, Japan, **7** Laboratory for Animal Resources and Genetic Engineering, RIKEN Center for Developmental Biology, Kobe, Japan

Abstract

Phosphatidylinositol binding clathrin assembly protein (PICALM), also known as clathrin assembly lymphoid myeloid leukemia protein (CALM), was originally isolated as part of the fusion gene *CALM/AF10*, which results from the chromosomal translocation t(10;11)(p13;q14). CALM is sufficient to drive clathrin assembly *in vitro* on lipid monolayers and regulates clathrin-coated budding and the size and shape of the vesicles at the plasma membrane. However, the physiological role of CALM has yet to be elucidated. Here, the role of CALM *in vivo* was investigated using *CALM*-deficient mice. *CALM*-deficient mice exhibited retarded growth *in utero* and were dwarfed throughout their shortened life-spans. Moreover, *CALM*-deficient mice suffered from severe anemia, and the maturation and iron content in erythroid precursors were severely impaired. *CALM*-deficient erythroid cells and embryonic fibroblasts exhibited impaired clathrin-mediated endocytosis of transferrin. These results indicate that CALM is required for erythroid maturation and transferrin internalization in mice.

Citation: Suzuki M, Tanaka H, Tanimura A, Tanabe K, Oe N, et al. (2012) The Clathrin Assembly Protein PICALM Is Required for Erythroid Maturation and Transferrin Internalization in Mice. PLoS ONE 7(2): e31854. doi:10.1371/journal.pone.0031854

Editor: Tsutomu Kume, Feinberg Cardiovascular Research Institute, Northwestern University, United States of America

Received August 1, 2011; **Accepted** January 17, 2012; **Published** February 21, 2012

Copyright: © 2012 Suzuki et al. This is an open-access article distributed under the terms of the Creative Commons Attribution License, which permits unrestricted use, distribution, and reproduction in any medium, provided the original author and source are credited.

Funding: This work was supported by research grants from the Ministry of Education, Science, Sports, Culture and Technology, Japan; Kurokawa Cancer Research Foundation; The Japan Health Foundation; The Naito Foundation; Sasakawa Scientific Research Grant from The Japan Science Society; and Nara Women's University Intramural Grant for Project Research. The funders had no role in study design, data collection and analysis, decision to publish, or preparation of the manuscript.

Competing Interests: The authors have declared that no competing interests exist.

* E-mail: toshiwatana@cc.nara-wu.ac.jp

Introduction

Clathrin-coated vesicles mediate endocytosis of plasma membrane receptors, channels, and transporters, as well as transmembrane proteins and various soluble macromolecules. As the main component of clathrin-coated pits and vesicles, clathrin forms structures termed triskelia, each composed of three heavy and three light chains [1–5], which in turn assemble into a lattice-like structure on the surface of coated pits. The major proteins that drive coated pit formation are the adaptor protein complex AP-2 [1,6,7] and clathrin assembly proteins such as phosphatidylinositol-binding clathrin assembly protein (PICALM), also known as clathrin assembly lymphoid myeloid leukemia protein (CALM). The neuronal homolog of CALM, AP180, has been shown to be sufficient for clathrin lattice assembly on lipid monolayers and for the regulation of clathrin-coated buds and the size and shape of vesicles at the plasma membrane [8–11].

CALM possesses an AP180 N-terminal homology (ANTH) domain that binds to membrane lipids [9,12–15] and specific motifs that bind to clathrin and AP-2, which are the primary components of clathrin-coated vesicles [11,14,15]. Cellular depletion of CALM by RNA interference results in the formation of clathrin-coated structures of abnormal size and shape, which suggests that CALM regulates the proper formation of clathrin-coated vesicles [11].

CALM was originally isolated as a fusion gene, *CALM/AF10*, which results from the chromosomal translocation t(10;11)(p13;q14). This translocation is a cytogenetic abnormality found in acute lymphoblastic leukemia, acute myeloid leukemia and in malignant lymphomas [16]. In a murine bone marrow transplantation model, expression of *CALM/AF10* in primary murine bone marrow cells results in the development of an aggressive form of leukemia [17,18]. These data suggest that CALM may play an important role in the growth and differentiation of hematopoietic cells. This notion is supported by reports that *fit1* mutants, which contain nonsense point mutations in the *CALM* gene, are anemic, display numerous peripheral blood defects, and are deficient in early hematopoietic progenitor cell populations [19–23]. Detailed analysis of the hematopoietic defects of *fit1* mutants has yet to be reported, and so the physiological role of CALM remains elusive.

Using a genetic approach to elucidate the function of CALM in mammals, we established *CALM*-deficient mice through gene

targeting. *CALM*-deficient mice were growth retarded *in utero* and remained dwarfed throughout their shortened life-span. In addition, *CALM*-deficient mice suffered from severe anemia due to ineffective erythropoiesis in the bone marrow. These phenotypes resembled those of *fit1* mutants. Moreover, the maturation and iron content of erythroid precursors were severely impaired in *CALM*-deficient mice. In addition, erythroid cells and murine embryonic fibroblasts (MEFs) isolated from *CALM*-deficient mice exhibited impaired clathrin-mediated internalization of transferrin. These data collectively demonstrate that CALM is required for erythroid maturation and transferrin internalization in mice.

Materials and Methods

Ethics Statement

This study received specific approval from the Committee of Animal Experiments, Nara Women's University (approval ID 06-13).

Generation of *CALM*-deficient mice

A genomic clone encompassing the exon that contained the initiation codon (methionine) of *CALM* was isolated from a C57BL/6 BAC library (BACPAC) using Red/ET methods. A targeting vector was constructed in which the marker gene PGK-neo-pA was inserted into this exon. A DT-A fragment was ligated to the 5′ end of the targeting vector for negative selection. The targeting vector was linearized by *Sal* I digestion and introduced into TT2 embryonic stem (ES) cells by electroporation [24]. Of 96 G418-resistant clones, 22 were positive for homologous recombination, as determined by PCR (http://www.cdb.riken.jp/arg/Methods.html), eight clones had undergone homologous recombination as determined by Southern blot analysis. Three clones were injected into 8-cell stage embryos. Chimeras were mated with C57BL/6J females and germline transmission of the disrupted *CALM* allele was confirmed. Heterozygous F1 mice were intercrossed to produce homozygous *CALM*-deficient mice (Acc. No. CDB0683K: http://www.cdb.riken.jp/arg/mutant%20mice%20list.html). Genotyping was carried out using PCR and specific primers designed to amplify either the mutant or wild-type allele. The sequences of the primers used for PCR analysis were as follows: primer A: 5′-ATGTCTGGCCAGAGCCTGACGGACCGAATC-3′ and calm typing C: 5′-GGGTCGGGAGAGGATGCGGGGGGTCTTCAC-3′ for the wild-type allele; and Neogt-1: 5′-CTGACCGCTTCCTCGTGCTTTACG-3′ and calm typing C for the knockout allele.

Antibodies

For analysis by fluorescence-activated cell sorting (FACS), the following antibodies were purchased from BD Pharmingen: anti-c-Kit (2B8), -Sca-1 (D7), -TER119 (specific for erythroid lineage cells), -Mac-1 (M1/70), -Gr-1 (RB6-8C5), -CD11c (HL3), -B220 (RA3-6B2), -CD44 (IM7), and -CD3e (145-2C11). For immunohistochemistry, an anti-transferrin receptor antibody was purchased from Zymed. Alexa488-conjugated anti-mouse IgG was obtained from Invitrogen. For immunoblot analysis, an anti-β-actin antibody was purchased from Sigma, the anti-CALM polyclonal antibody (G-17) was purchased from Santa Cruz, and the horseradish peroxidase (HRP)-conjugated anti-mouse IgG and anti-goat IgG antibodies were purchased from Thermo Fisher Scientific.

Immunoblot Analysis

Immunoblot analysis was performed as described previously [25]. Briefly, cells were lysed in SDS-PAGE sample buffer, separated by SDS-PAGE, and then transferred to a nitrocellulose membrane. The membranes were incubated in blocking buffer (140 mM NaCl, 1 mM EDTA, and 20 mM Tris-HCl, pH 7.4) containing 5% bovine serum albumin and 0.02% Tween 20, followed by incubation for 1 h at room temperature with primary antibody. Membranes were incubated with the appropriate secondary antibodies diluted in blocking buffer, and then immunoreactive proteins were visualized by enhanced chemiluminescence (GE Healthcare).

Flow cytometry

Flow cytometry were performed using a BD FACS Canto II system (BD Biosciences). The data were analyzed using BD FACSDiva software (BD Biosciences) or FlowJo software (TreeStar, Ashland, OR).

Purification of murine Lin^- $Sca\text{-}1^+$ $c\text{-}Kit^+$ (LSK) cells

Murine fetal liver (FL) cells were harvested from embryonic day 14.5 (E14.5) embryos and mononuclear cells (MNCs) were obtained by density gradient centrifugation. MNCs were incubated with a cocktail of anti-lineage antibodies (Abs): biotinylated anti-CD3e (145–2C11), -CD45R/B220 (RA3–6B2), -Gr-1 (RB6–8C5), and -TER-119 (TER-119) Abs; fluorescein isothiocyanate (FITC)-conjugated anti-Sca-1 (D7); allophycocyanin (APC)-conjugated anti-c-Kit (2B8); and streptavidin-PE-cy7 (BD Biosciences). LSK cells were obtained by FACS using FACS Aria (BD Biosciences). Staining with 7-amino-actinomycin D (Calbiochem) was used to eliminate non-viable cells.

Hematopoietic stem cell (HSC) transplantation

LSK cells (1×10^6) obtained from the fetal livers of *CALM*-deficient and wild-type E14.5 embryos (CD45.2) were transferred into irradiated (1.300 rad) recipients along with 1×10^5 wild-type LSK cells (CD45.1). The relative contributions from the transferred HSCs were analyzed 9 weeks after transplantation.

Analysis of intracellular labile iron pool (LIP)

Cellular LIP was measured using the fluorescent metalosensor calcein-AM(CA-AM; Invitrogen), as previously reported, with some modifications [26,27]. Briefly, cells were incubated for 1 h with or without 500 μM deferoxamine (DFO) (Sigma) in serum-free media (α-MEM). Following washing with phosphate-buffered saline (PBS), cells were incubated with 250 nM CA-AM for 10 min at 37°C in PBS, washed twice, and then resuspended at a density of 1×10^6/mL in PBS containing 1% bovine serum albumin at room temperature. In addition to CA-AM, as indicated, cells were also incubated with APC-conjugated anti-TER119 and PE-conjugated anti-CD71 Abs. Fluorescence intensity was measured using FACS Canto II (BD Biosciences) in continuous mode. LIP was calculated as the difference in CA mean fluorescence intensity between DFO-treated and -untreated cells.

Image analysis

Microscopic images of May-Grunwald-Giemsa-stained peripheral smears were obtained using an Olympus (BX51) microscope equipped with a digital camera (Olympus DP71) and processed with DP Controller software.

CALM-deficient embryonic fibroblastoid cell lines

Primary MEFs were generated from mated wild-type or *CALM*-deficient mice 14.5 days after conception. Primary MEFs were immortalized by transfection with a plasmid containing SV40 genomic DNA. Briefly, primary MEFs were plated in six-well

plates and transfected with 1 μg of total DNA using Lipofectamine 2000 Reagent (Invitrogen, CA), according to the manufacturer's instructions. Stable immortalized cell clones were obtained by serial dilution. The expression of CALM protein was assessed by immunoblot. MEFs were cultured in Dulbecco's modified Eagle's medium (DMEM) supplemented with 10% fetal calf serum (FCS) and antibiotics (penicillin/streptomycin) at 37°C and 5% CO_2.

Internalization assay

To evaluate the uptake of transferrin by erythroblasts, single cell suspensions from fetal liver or bone marrow were incubated in serum-free medium at 37°C for 2 h.

Cells were labeled with 50 μg/ml Alexa Fluor 647-conjugated human transferrin (Invtrogen) in binding buffer (RPMI1640 containing 20 mM HEPES pH 7.4, 1% BSA) on ice for 30 min. After washing to remove unbound transferrin, internalization of transferrin was induced by incubating the cells in buffer (RPMI1640 containing 10% fetal bovine serum) at 37°C for various times. Any transferrin that remained bound to the plasma membrane was removed by incubating the cells in pre-chilled acidic buffer (20 mM MES pH 5, 130 mM NaCl, 50 μM deforoxamine, 2 mM $CaCl_2$ and 0.1% BSA) on ice for 20 min. After washing three times, cells were labeled with FITC-conjugated anti-TER119 Ab and the fluorescence intensity of internalized transferrin in the erythroblast cell population (TER119-high cells) was quantified by FACS Canto II (BD Biosciences).

To detect the internalization of transferrin in MEFs, cells on coverslips were incubated with 10 μg/ml Alexa Fluor 488-conjugated human transferrin (Invitrogen) for 20 min at 37°C, and then fixed with 3.7% formaldehyde in PBS for 15 min at room temperature. After washing with PBS, cover slips were mounted on glass slides using Prolong Gold (Invitrogen) and then analyzed by spinning disc confocal microscopy (CSU10; Yokogawa Electric Co.) using an inverted microscope (IX-71; Olympus) equipped with an Ar/Kr laser, as described previously [25]. To quantitate the internalization of transferrin in MEFs, the fluorescence intensity of randomly selected individual cells (total cell area) was measured and processed using Image J software (http://rsbweb.nih.gov/ij/index.html).

Results

Generation of *CALM*-deficient mice

To address the functional role of CALM in mice, *CALM*-deficient mice were generated using a gene targeting approach. The *CALM*-targeting construct was designed with an expression cassette containing the neomycin-resistance gene (*neo*^{r}) inserted just after the initiation ATG codon in exon 1 of the *CALM* gene (Fig. 1A). Eight clonal ES cell lines bearing the targeted allele were identified by Southern blot analysis, of which three were used to generate chimeric mice with germ line transmission of the targeted *CALM* allele. Their offspring were used for all studies reported herein. Heterozygous mice exhibited no obvious abnormalities. To generate homozygous *CALM*-deficient mice, F1 heterozygous mice were interbred and the F2 offspring were genotyped by PCR and Southern blot (Fig. 1B and C). The absence of CALM protein expression in *CALM*-deficient mice was confirmed by immunoblot (Fig. 1D).

CALM-deficient mice exhibit significant growth defects and a shortened life-span

CALM-deficient mice were obtained at the expected Mendelian ratios (Table 1). The *CALM*-deficient mice were smaller in size compared to their wild-type littermates (Fig. 2A), and more than 90% died between birth and weaning (Table 1). To characterize the retarded growth phenotype of *CALM*-deficient mice in more detail, the body weight of *CALM*-deficient mice and their wild-type littermates was assessed. As shown in Figure 2B, *CALM*-deficient mice weighed, on average, 35.3% (for males) and 39.7% (for females) of the weight of normal littermates at weaning (28 days of age). Because *CALM*-deficient mice exhibited a growth retardation phenotype at birth, we also assessed whether *CALM* was necessary for normal prenatal growth. The weight of *CALM*-deficient embryos was compared to that of their wild-type littermates at E14.5. *CALM*-deficient embryos were approximately 74% of the size of normal littermates (data not shown), which suggested that *CALM* is also required for normal prenatal growth. The phenotype of *CALM*-deficient mice therefore was retarded growth *in utero* with mice remaining dwarfed throughout their life-span.

It should be noted that after back-crossing five times with C57B6/J mice, no *CALM*-deficient mice were obtained, which suggested that *CALM* deficiency may result in a lethal phenotype that is dependent on the genetic background of B6 and CBA mice.

CALM-deficient mice suffer from severe anemia

Many of the tissues in *CALM*-deficient mice, including liver, kidney and tibia, were smaller compared to wild-type mice (Fig. 2C, E). By marked contrast, however, the spleens of *CALM*-deficient mice were larger than those of their wild-type littermates, which was indicative of splenomegaly (Fig. 2D). Histologic examination revealed that follicles were absent in the spleens of *CALM*-deficient mice, which indicating a defect in the B cell population. This was confirmed by FACS analysis, which was consistent with impaired B cell maturation in the spleens of *CALM*-deficient mice (data not shown). In addition, there were fewer bone marrow cells in *CALM*-deficient mice and the isolated cell pellets were pale in appearance (Fig. 2F), which suggested a defect in the regulation of hematopoiesis. In fact, the number of TER119-positive erythroid cells in the bone marrow of *CALM*-deficient mice was significantly reduced compared to control littermates (Fig. 2G). We also observed a ballooning and granular degeneration of hepatocytes (data not shown), indicative of hepatocyte damage. As shown in Table 2, the number of red blood cells (RBCs) in *CALM*-deficient mice was significantly reduced compared to control littermates, and the mice were severely anemic, with dramatically lower hemoglobin levels. Additionally, peripheral blood in *CALM*-deficient mice contained hypochromic RBCs (Fig. 2H).

Maturation of erythroid cells is impaired in *CALM*-deficient mice

To investigate whether the severe anemia in *CALM*-deficient mice was due to defects in erythroid differentiation, the expression of transferrin receptor 1 (CD71) and TER119 was analyzed by FACS, which allows the different stages of maturation of murine erythroblasts to be distinguished [28]. Bone marrow cells were immunostained with FITC-conjugated anti-TER119 and PE-conjugated CD71 Abs (Fig. 3A, C). A representative FACS histogram is shown in Figure 3A. Region I of the histogram ($CD71^{high}TER119^{low}$) represents the proerythroblast population or immature erythroblasts. Region II ($CD71^{high}TER119^{high}$) represents the basophilic erythroblast population. Region III ($CD71^{low\text{-}med}$ $TER119^{high}$) represents the polychromatic and orthochromatic erythroblast populations, which are hemoglobin-producing cells, and region IV ($CD71^{low}TER119^{high}$) represents mature erythrocytes. This profile is known as Socolovsky's plot. As shown in Figure 3A and C, *CALM*-deficient mice had significantly fewer cells in region II compared with their wild-type littermates. These results

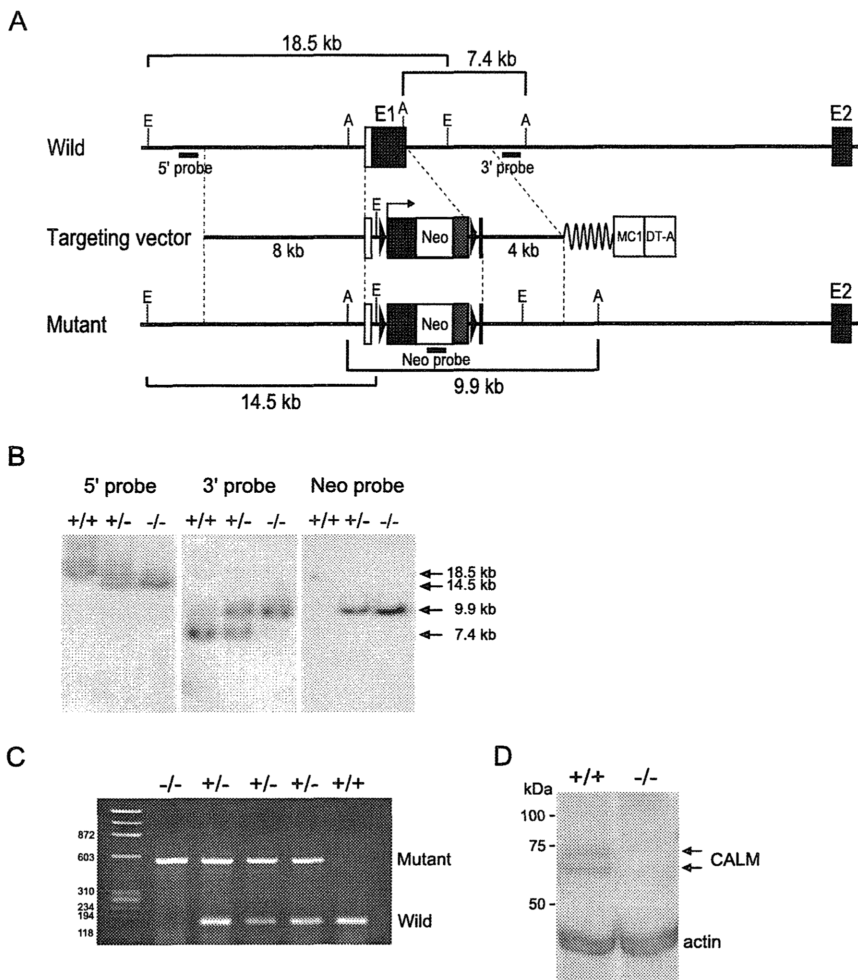

Figure 1. Targeted disruption of the *CALM* gene. (A) Schematic of the targeting strategy used for disruption of the first coding exon of *CALM*. (B) Southern hybridization analysis of DNA isolated from targeted mouse embryos. From left to right: 5′ probe, 3′ probe and neo probe, as shown in A. (C) Genomic PCR analysis of DNA isolated from mouse tail. The genotypes are indicated above each lane. (D) Immunoblot analysis of stable MEF cell lines from wild-type (+/+) and *CALM*-deficient (−/−) mouse embryos (E14.5). The expected molecular weights of CALM are 62 and 72 kDa (arrows). Actin was used as a loading control.
doi:10.1371/journal.pone.0031854.g001

suggested that erythroid maturation at the stage of proerythroblast to immature erythroblast is impaired in *CALM*-deficient mice.

To confirm these results, we also analyzed the expression levels of CD44 and TER119, the relative levels of which have been shown to correlate with different maturation stages of murine erythroblasts [29]. Bone marrow cells were subjected to immuno-staining with FITC-conjugated anti-TER119 and APC-conjugated CD44 Abs (Fig. 3 B, D). As shown in Figure 3B and D, *CALM*-deficient mice had significantly lower numbers of cells in region III compared with their wild-type littermates, which supported the idea that erythroid maturation from proerythroblast to immature erythroblast is impaired in *CALM*-deficient mice.

These data collectively suggested that the maturation of erythroid cells is severely impaired in *CALM*-deficient mice.

Table 1. Genotypes of intercrossed CALM$^{+/-}$ mice.

Stage	+/+	+/−	−/−
P28	72 (69)	138	8 (69)
P0	23 (25)	50	8 (25)
E19.5	9 (9)	17	6 (9)
E18.5	16 (13)	26	12 (13)
E14.5	17 (15)	29	18 (15)

The total number of embryos or postnatal mice isolated for each genotype is indicated, with values in parentheses indicating the number of embryos or postnatal mice expected based on Mendelian distribution.
doi:10.1371/journal.pone.0031854.t001

The erythroid defects in *CALM*-deficient mice are cell autonomous

HSC activity was analyzed by transplantation assay. Fetal liver cells from wild-type or *CALM*-deficient embryos (CD45.2) were transplanted into X-ray irradiated host mice along with a one-tenth fraction of wild-type cells (CD45.1) as a competitor. After 9 weeks, CD45.2-positive hematopoietic cells derived from *CALM*-deficient embryos had repopulated the bone marrow at the same rate as wild-type cells (Fig. 4A). However, after 12 weeks, impaired maturation of early to late stage erythroblasts and abnormal erythroid cells were observed only in host mice transplanted with fetal liver cells from *CALM*-deficient embryos (Fig. 4B and C). The

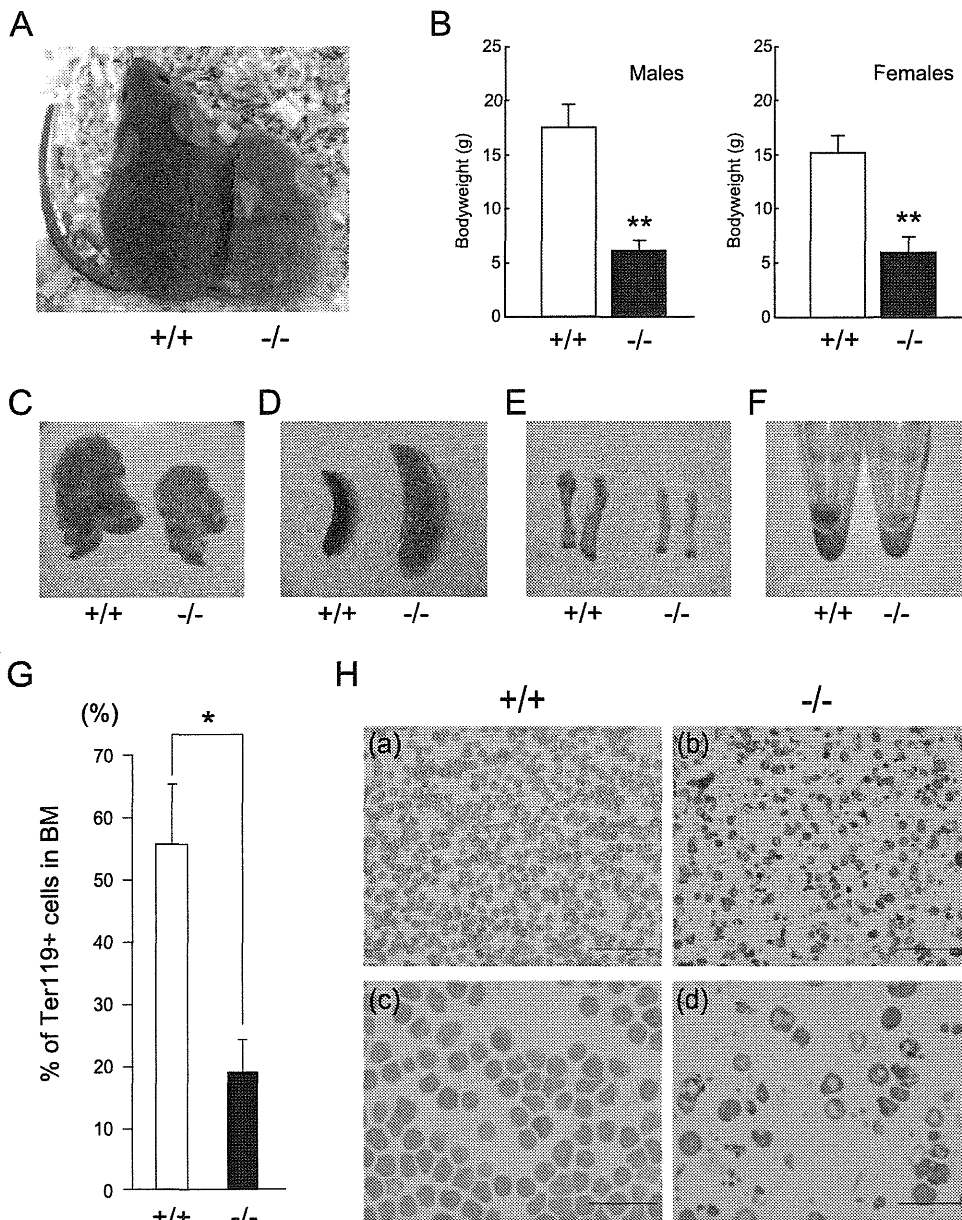

Figure 2. Growth retardation and peripheral blood morphology in postnatal *CALM*-deficient mice. (A) Wild-type (+/+) (left) and *CALM*-deficient (−/−) (right) mice at 3 weeks of age. (B) Average weight of wild-type (+/+) and *CALM*-deficient (−/−) mice at postnatal day 28. Data shown represent *CALM*-deficient males (n = 3), *CALM*-deficient females (n = 4), wild-type males (n = 36), and wild-type females (n = 35). **, $P<0.01$ vs control. Liver (C), spleen (D) and tibia (E) from wild-type (+/+) or *CALM*-deficient (−/−) mice at 3 weeks of age. (F) Bone marrow cells were collected by centrifugation. Note that the pellet from *CALM*-deficient (−/−) mice is small and pale in color. (G) Quantification of TER119-positive bone marrow cells (data represent means±SD; n = 5). *, $P<0.05$ vs. control. (H) Peripheral blood smears from wild-type (+/+) littermates (left panels, a and c) or *CALM*-deficient (−/−) mice (right panels, b and d) at 3 weeks of age. Magnification: upper panels, 400×; lower panels, 1000×. Scale bar, 50 μm (upper panel) and 20 μm (lower panel).
doi:10.1371/journal.pone.0031854.g002

impaired maturation of erythroid cells was confirmed by anti-CD44 staining (data not shown).

In addition, host mice transplanted with fetal liver cells from *CALM*-deficient embryos were anemic and had fewer RBCs and lower hemoglobin levels than wild-type transplanted mice (data not shown). These results indicated that the observed erythroid defects in *CALM*-deficient mice were cell autonomous and not a result of the hematopoietic environment.

It should be noted that host mice transplanted with fetal liver cells from *CALM*-deficient embryos also exhibited splenomegaly, and that there was a similar pattern of progenitor activity in spleen cells as in bone marrow (data not shown). On the other hand, no progenitor activity was detected in spleen cells from host mice transplanted with fetal liver cells from wild-type embryos.

Incorporation of iron is reduced in erythroid cells of *CALM*-deficient mice

Erythroid cells from *CALM*-deficient mice were severely anemic and erythroid maturation was impaired (Fig. 2, 3 and 4). Since iron deficiency is known to inhibit erythroid differentiation and

Table 2. Hematopoietic parameters of control and CALM$^{-/-}$ mice.

Genotype	WBC	RBC	Hb	HCT	MCV	MCH	MCHC	PLT
+/+	3.7±0.98	875.3±65.5	13.2±0.85	47.4±3.29	54.1±0.44	15.0±0.18	27.8±0.17	80.0±54.45
+/−	2.3±0.49	840.0±52.4	12.6±0.88	46.5±2.42	55.4±2.13	15.0±0.97	27.1±0.74	103.0±29.90
−/−	3.4±0.90	267.8±97.0	3.7±1.29	14.2±4.71	53.4±4.80	13.9±1.17	26.1±1.01	118.6±23.34

Data were obtained from 3-week-old mice. WBC, white blood cell count ($\times 10^3/\mu l$); RBC, red blood cell ($\times 10^4/\mu l$); Hb, hemoglobin (g/dl); HCT, hematocrit (%); MCV, mean corpuscular volume (fl); MCH, mean corpuscular hemoglobin (pg); MCHC, mean corpuscular hemoglobin concentration (g/dl); Plt, platelet count ($\times 10^4/\mu l$). Data are the mean ± SD of four wild-type, four CALM$^{+/-}$, and five CALM$^{-/-}$ mice. Statistical analysis was carried out using the unpaired t-test. **$P<0.01$, *$P<0.05$.
doi:10.1371/journal.pone.0031854.t002

induce anemia [30,31], we investigated whether an iron-deficiency in erythroid cells in *CALM*-deficient mice was the cause of the anemia.

Iron bound to transferrin is taken up by cells via transferrin receptor 1-mediated endocytosis. This is the main pathway of iron intake in erythroid cells. We first analyzed amount of ferritin and transferrin in the plasma of wild-type and *CALM*-deficient mice by ELISA (ICL, Portland, OR, USA). There were no differences in the levels of transferrin in wild-type and *CALM*-deficient mice, whereas ferritin levels, which directly correlate with the total amount of iron stored in the body, were three-times higher in *CALM*-deficient mice than wild-type mice. These results suggested that there was an excess of iron in the body of *CALM*-deficient mice, despite the hypochromic and microcytic anemic phenotype. This suggested that there was an imbalance in the distribution of iron from erythroid cells to other tissues in *CALM*-deficient mice. To investigate this possibility, we examined the labile (or chelatable) iron pool (LIP) in erythroid cells, which is a point of convergence of the iron metabolic pathways. The LIP was measured using the cell permeable iron chelator CA-AM, as previously described [26,27]. Upon uptake by viable cells, CA-AM undergoes hydrolysis by esterases to form calcein (CA), the fluorescence of which can be measured (excitation wavelength of 488 nm, emission wavelength of 517 nm). CA fluorescence is quenched upon binding to the cellular LIP in a stoichiometric fashion. The presence of a high-affinity chelator such as desferoxamine (DFO) results in extraction of iron from CA-iron complexes and a corresponding increase in CA fluorescence. Thus, the difference in cellular fluorescence in the presence and absence of DFO can be taken as a measure of the LIP. The LIP is dependent on cell type and maturation stage; analysis of erythroid cells in the blood, bone marrow and in culture has shown that the LIP decreases during maturation [26,27]. Compared to wild-type cells, erythroid cells in the bone marrow of *CALM*-deficient mice exhibited higher CA fluorescence intensity in regions I through III of the Socolovsky plot (Fig. 5A, B). As shown in Fig. 5C and D, the mean fluorescence intensity (MFI) of CA-AM-loaded wild-type fetal liver erythroid cells at stages I and II was 762 and 126, respectively, and MFI was significantly increased to 1211 and 263, respectively, by treatment with DFO. Based on the difference in MFI in DFO-treated and -untreated cells, the LIP in wild-type cells in stages I and II was 484±181 and 137±17 (MFI±S.D; n = 7), respectively (Fig. 5E). On the other hand, in *CALM*-deficient cells, there was only a small increase in CA fluorescence in the presence of DFO, which suggested that the cellular LIP in *CALM*-deficient cells was smaller than in wild-type cells. The LIP also appeared to be relatively constant in *CALM*-deficient cells (55±76 and 39±26 at stages I and II, respectively; n = 3). Similar results were obtained using bone marrow cells from host mice transplanted with fetal liver cells from wild-type or *CALM*-deficient embryos (data not shown).

Several reports show that CA is pumped out of cells via the multidrug resistance machinery [32]. There were no apparent differences in mean CA-fluorescence intensity in DFO-treated wild-type and *CALM*-deficient cells, which indicated that there were similar levels of CA in both cell types (Fig. 5 D). Thus, it is unlikely that the differences in LIP were due to the multidrug resistance machinery. Taken together, these results indicated that the iron content of erythroid cells at stages I and II is lower in *CALM*-deficient mice compared to their wild-type littermates. Therefore, altered distribution of iron in *CALM*-deficient mice inhibits erythroid maturation and results in anemia.

Reduced incorporation of transferrin into erythroid cells and MEFs derived from *CALM*-deficient mice

Transferrin receptor 1, also known as CD71, is highly expressed in erythroblasts, and uptake of iron-bound transferrin through transferrin receptor 1 is the main pathway of iron uptake in erythroid precursors [33,34]. It is also well established that inhibition of this process inhibits erythroid maturation. Because transferrin is internalized via clathrin-dependent endocytosis [6,35], and CALM localizes to clathrin-coated pits, clathrin-mediated endocytosis of transferrin in *CALM*-deficient mice was assessed [11,15].

Transferrin uptake by erythroid cells from fetal liver was assessed by FACS, as described in Materials and Methods. The level of transferrin receptor (CD71) expression in TER119-positive erythroid cells from *CALM*-deficient mice was about 2.5-fold higher than that seen in wild-type cells (3365±1398 and 8554±1681 MFI±S.D, respectively; n = 3), which could reflect differences in the internalization of transferrin receptors. Thus, transferrin uptake was normalized to transferrin receptor level for this analysis. In wild-type cells, 62% of bound transferrin was rapidly internalized after 3 min. On the other hand, only 19% of bound transferrin was internalized by *CALM*-deficient cells (Fig. 6A). Similar results were obtained using wild-type and *CALM*-deficient erythroid cells derived from neonatal bone marrow (data not shown).

To examine this defect in transferrin internalization in more detail, MEFs were established from wild-type and *CALM*-deficient E14.5 embryos. Wild-type MEFs expressed the transferrin receptor and transferrin was internalized in a constitutive manner (Fig. 6B). However, *CALM* knock-out MEFs derived from *CALM*-deficient embryos failed to incorporate transferrin (Fig. 6B), despite similar overall levels of transferrin receptor (Fig. 6C). Transferrin uptake in wild-type and *CALM*-deficient MEFs was quantitated and the results are shown in Fig. 6D. Uptake of transferrin by wild-type MEFs was approximately twice that seen in *CALM*-deficient cells. These results indicated that the internalization of transferrin receptors is abrogated in *CALM*-deficient cells. Thus, the erythropoietic defects in *CALM*-deficient mice may be due to inhibition of transferrin endocytosis in the absence of CALM.

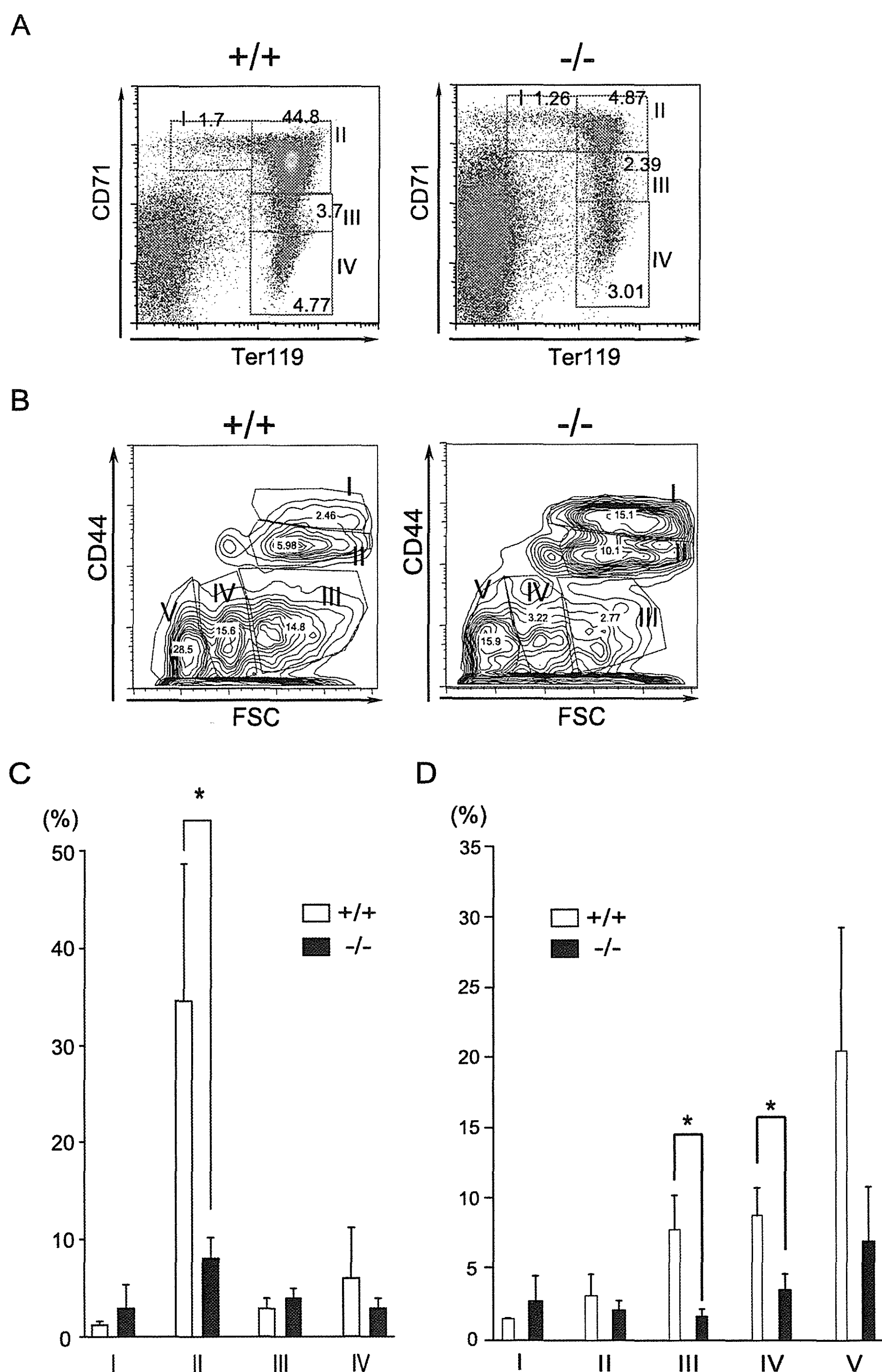

Figure 3. FACS analyses of erythroblasts at different stages of maturation in wild-type or *CALM*-deficient mice. (A) Representative flow cytometry histograms. In 3-week-old mice, erythroblasts at different maturation stages were identified by double staining with FITC-conjugated anti-TER119 and PE-conjugated anti-CD71 Abs. (B) Representative flow cytometry histograms. Erythroblasts at different maturation stages were identified by double staining with FITC-conjugated anti-TER119 and APC-conjugated anti-CD44 Abs. Plots of CD44 vs. forward scatter (FSC) for TRE119-positive cells are shown. (C) Quantification of regions I to IV of (A) (data represent means±SD; n = 4). *, $P<0.05$ vs. control. (D) Quantification of regions I to V of (B) (data represent means±SD; n = 5). *, $P<0.05$ vs. control.
doi:10.1371/journal.pone.0031854.g003

Discussion

In this report, we established *CALM*-deficient mice and showed that these mice exhibit retarded growth *in utero* and remain dwarfed throughout their shortened life-span. *CALM*-deficient mice suffer from severe anemia, similar to what has been reported for *fit1* mutant mice [21]. In addition, the maturation of erythroid precursors was severely impaired in mice lacking CALM. The iron content of erythroid precursors was lower in *CALM*-deficient mice compared to their wild-type littermates. Importantly, those

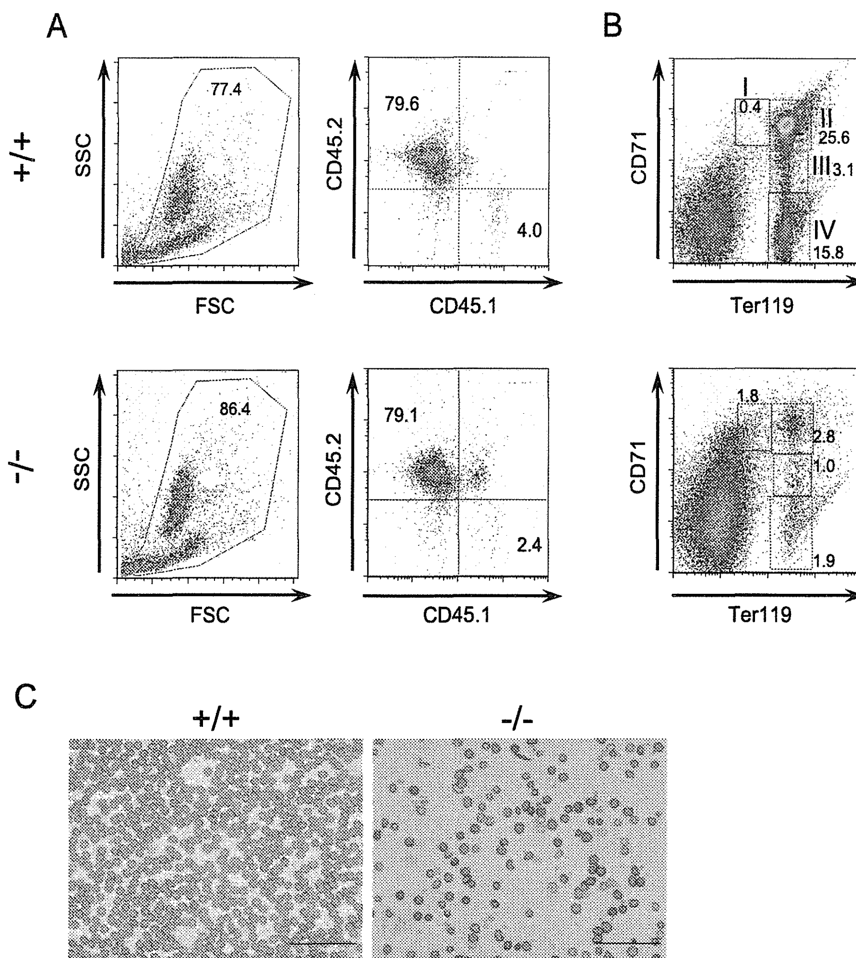

Figure 4. *CALM* is required for normal erythropoiesis. (A) CD45 profile of peripheral blood cells from transplanted mice 9 weeks after transplantation. (B) FACS analyses of erythroblasts at different maturation stages from transplanted mice using anti-TER119 and anti-CD71 Abs. (C) Peripheral blood smears from mice transplanted with fetal liver cells from either wild-type littermates or *CALM*-deficient embryos. Scale bar, 50 μm. In A, B, and C, (+/+) and (−/−) represent host mice transplanted with cells from wild-type and *CALM*-deficient mice, respectively.
doi:10.1371/journal.pone.0031854.g004

phenotypes were reconstituted in transplantation experiments. The amount of ferritin in *CALM*-deficient mice was three-times higher than that in wild-type mice, suggesting that there is an excess of iron in the plasma of mice deficient in CALM.

It is well established that iron deficiency inhibits erythroid maturation [26,27,33,34]. Anemia is the most obvious manifestation of iron deficiency due to the large amount of iron required for hemoglobin production in developing erythroid cells. *Transferrin receptor 1*-deficient mice die during embryogenesis due to the lack of transferrin-mediated iron uptake [31]. Slc11a2 is the only transmembrane transporter protein known to be required for iron entry into cells and is required for normal hemoglobin production during the development of erythroid precursors. *Slc11a2*-deficient mice also exhibit severe anemia after birth [30]. Our results suggest that iron deficiency in *CALM*-deficient mice results in inhibition of erythroid maturation and subsequent anemia.

The question then arises as to which molecule involved in iron uptake is affected by *CALM*-deficiency in mice. Transferrin receptor 1 (TFR1), also known as CD71, is one such candidate molecule. TFR1 is highly expressed in erythroblasts, and the uptake of iron-bound transferrin through TFR1 is the main pathway by which iron enters erythroid precursors [33,34]. It is also well established that inhibition of this process prevents erythroid maturation due to iron deficiency [31]. Transferrin is taken up by cells through clathrin-dependent endocytosis [6,35]; thus, it is likely that impaired transferrin endocytosis in *CALM*-deficient mice underlies the inhibition of erythroid maturation. However, the involvement of CALM in clathrin-dependent endocytosis of transferrin remains controversial. While one study has shown that over-expression of full-length CALM and CALM fragments that contain clathrin-binding domains can block transferrin endocytosis [15], another study reports that over-expression of CALM had no effect on transferrin endocytosis [36]. CALM depletion experiments using small inhibitory (si)RNA did not demonstrate an effect on transferrin endocytosis, although there was partial inhibition of epidermal growth factor (EGF) receptor endocytosis [36,37]. Based on these reports, CALM is not believed to be an essential component of clathrin-associated endocytosis of transferrin [11,36,37]. The *CALM*-deficient mice generated in the current study provided an excellent model system for probing the role of CALM in clathrin-dependent endocytosis of transferrin. Transferrin uptake by erythroid cells was analyzed by FACS, and the results suggested that transferrin uptake is significantly attenuated in *CALM*-deficient erythroid cells. We also established *CALM* knock-out (KO) MEFs from *CALM*-deficient embryos and clearly demonstrated that *CALM* KO MEFs fail to

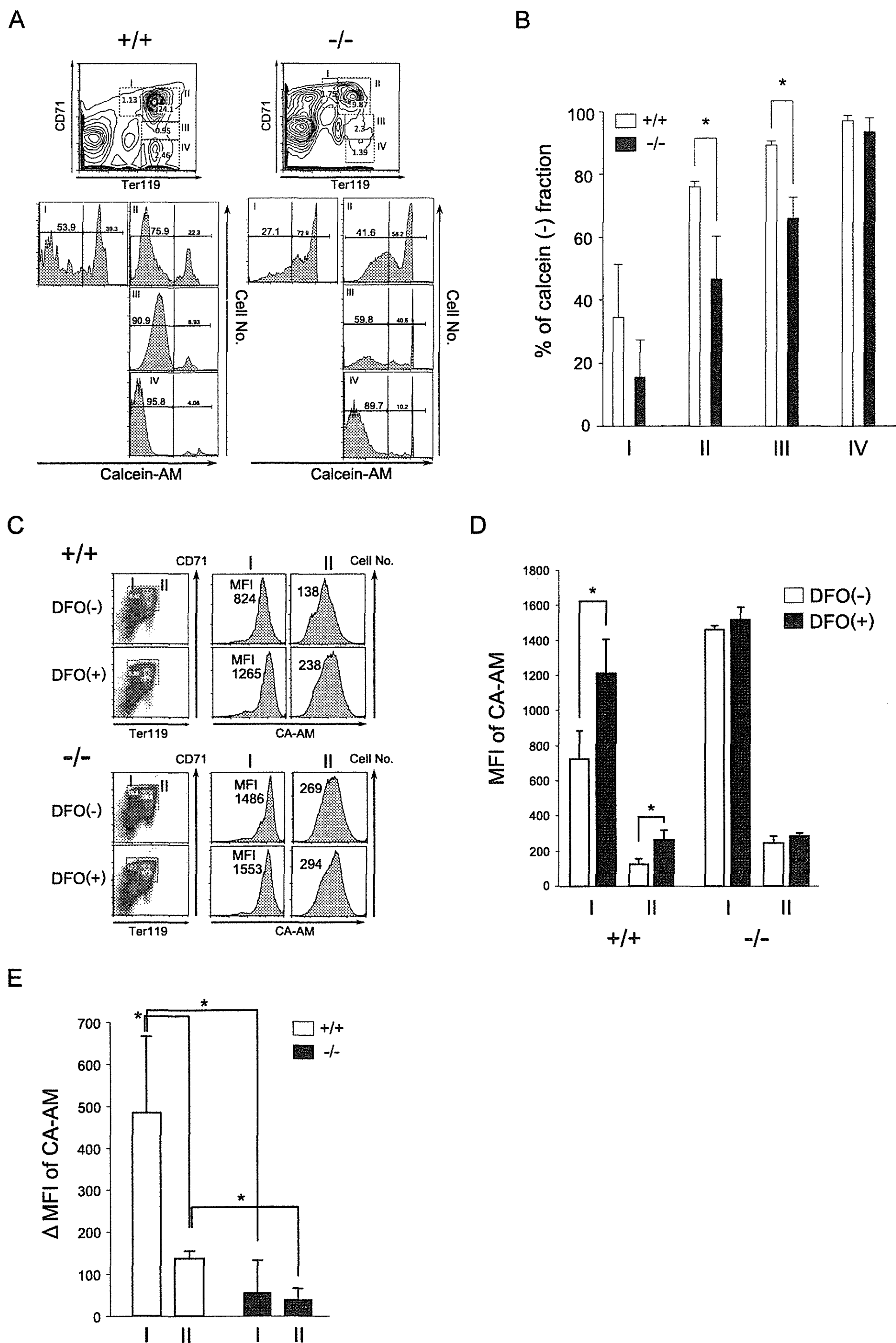

Figure 5. Flow cytometry analysis of the LIP. (A) Representative flow cytometry histograms. Erythroblasts at different stages of maturation were identified by double staining with APC-conjugated anti-TER119 and PE-conjugated anti-CD71 Abs (upper). These cells were simultaneously loaded with calcein (CA-AM) for the LIP assay (lower). (B) Quantification of CA-negative fractions in regions I to IV of (A) (data represent means±SD; n = 3). (C) Representative flow cytometry histograms of E14.5 fetal liver cells. Erythroblasts at different stages of maturation were identified by double staining with APC-conjugated anti-TER119 and PE-conjugated anti-CD71 Abs. Cells were treated for 1 h with the iron chelator DFO, loaded with CA-AM for 10 min, and then analyzed. (D) Representative fluorescence (FL1-high) histograms of CA-stained cells treated with or without DFO are shown, along with mean fluorescence intensity (MFI). (E) The LIP is represented by the difference in MFI between DFO-treated and -untreated cells (data represent means±SD; n = 3). *, $P<0.05$ vs. control. In A, B, C and D, (+/+) and (−/−) represent wild-type and *CALM*-deficient mice, respectively.
doi:10.1371/journal.pone.0031854.g005

A

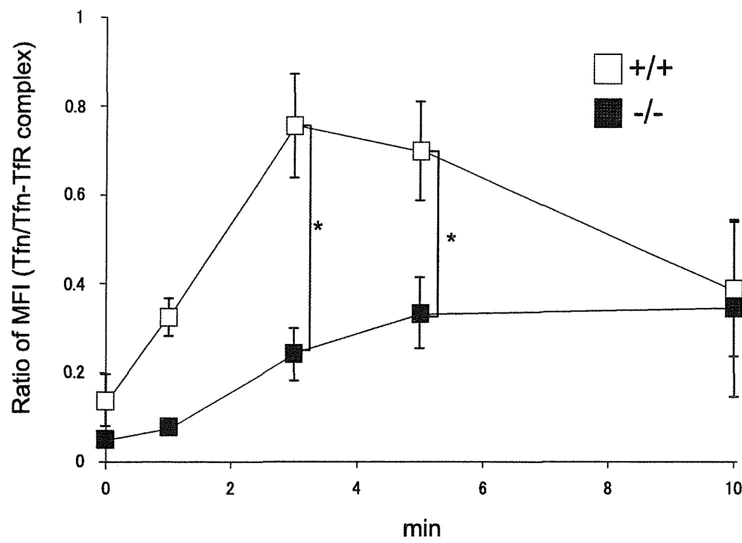

B

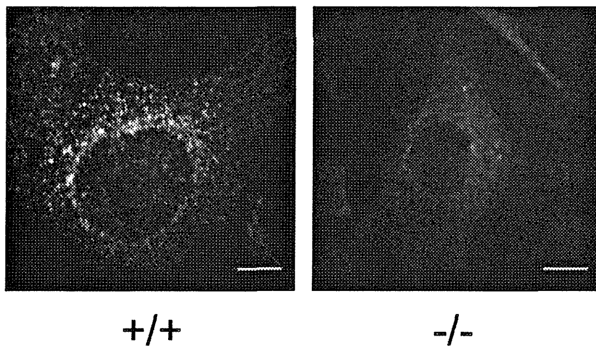

C

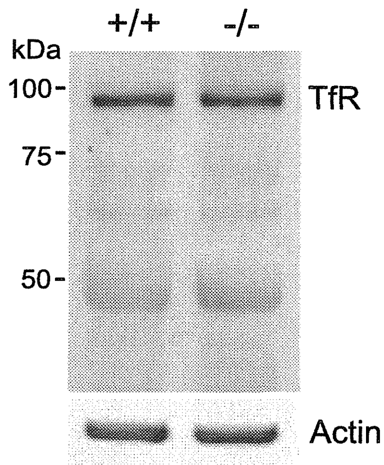

D

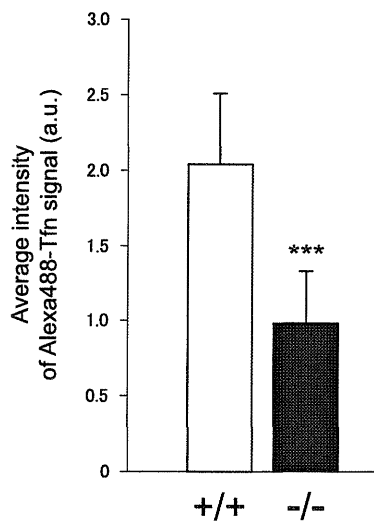

Figure 6. Impaired transferrin internalization in *CALM*-deficient erythroid cells and MEFs. (A) Uptake of transferrin in wild-type or *CALM*-deficient erythroid cells. Single cell suspensions from fetal livers were analyzed as described in Materials and Methods. Transferrin uptake was normalized to the ratio of mean anti-CD71 (transferrin receptor 1) fluorescence intensity between wild-type and *CALM*-deficient cells to control for

differences in transferrin receptor expression. (B) Uptake of transferrin by wild-type or *CALM*-deficient MEFs was analyzed as described previously [40]. Scale bar, 10 μm. (C) Expression of transferrin receptor 1 in wild-type and *CALM*-deficient MEFs was analyzed by immunoblot. Actin was used as a loading control. (D) Quantification of transferrin uptake was performed as described in Materials and Methods (data represent means±SD; n = 50 for wild-type cells and n = 54 for *CALM*-deficient cells). ***, $P<0.001$ vs. control. Fluorescence is shown in arbitrary units (*a.u.*). In A, B, C and D, (+/+) and (−/−) represent wild-type and *CALM*-deficient MEFs, respectively.
doi:10.1371/journal.pone.0031854.g006

incorporate transferrin. Thus, CALM does indeed appear to be involved in transferrin endocytosis in erythroid cells and MEFs. In addition, the LIP in erythroid cells, which represents a crossroads of iron metabolic pathways, was determined. The iron content of erythroid cells was lower in *CALM*-deficient mice compared to their wild-type littermates. Our results collectively suggest that defective transferrin endocytosis in *CALM*-deficient mice results in altered distribution of iron in the body and inhibition of erythroid maturation, resulting in an anemic state.

Discrepancies between the results obtained by RNA interference using cell lines and those derived from genetic models in mice are reported for several proteins involved in clathrin-mediated endocytosis, such as SMAP1, epsin1 and epsin 2 [36–42]. In these cases, impaired endocytosis was reported in response to the inhibition of protein expression by siRNA but not in gene-deficient mice. As suggested previously for other proteins, differences between our results and those of previous studies in terms of the involvement of CALM in transferrin endocytosis could be due to incomplete inhibition of protein expression using siRNA [36,37].

CALM was originally isolated as a component of the *CALM/AF10* fusion gene, which results from the chromosomal translocation t(10;11)(p13;q14) [16]. In a murine bone marrow transplantation model, expression of *CALM/AF10* in primary murine bone marrow cells results in the development of an aggressive form of leukemia [17,18]. These data suggest that CALM or clathrin-mediated endocytosis may play an important role in leukemogenesis. Recent reports demonstrate that the clathrin-binding domain of *CALM* is important for leukemogenesis by *CALM-AF10* [43,44]. The fact that deletion of *CALM* resulted in disruption of clathrin-mediated endocytosis of transferrin suggests that clathrin-mediated endocytosis may play a role in leukemogenesis. A number of other proteins that are important for hematopoiesis are substrates of clathrin-mediated endocytosis [45–47]. Thus, the *CALM*-deficient mice and MEFs established in this study will be useful tools for elucidating the involvement of *CALM* in leukemogenesis.

CALM plays an important role in the central nervous system (CNS). For example, reduction of CALM expression in hippocampal neurons results in dendritic dystrophy [48]. Although the current study focused mainly on hematological changes in *CALM*-deficient mice, we did some preliminary analyses of the mouse brain to assess any pathology of the neural system. Although there were no differences observed in the hippocampus and dentate gyrus between wild-type and *CALM*-deficient mice, there was significant atrophy of the cortex and ventricles were markedly enlarged in *CALM* -deficient mice (data not shown). A detailed analysis of these observations will be reported elsewhere.

In summary, our analysis of *CALM*-deficient mice supports an important role for CALM in erythroid maturation and transferrin incorporation via clathrin-dependent endocytosis. A number of other proteins that are important for hematopoiesis are also incorporated into cells via clathrin-mediated endocytosis [45–47]; thus, *CALM*-deficient mice and MEFs established from these mice should prove to be useful for studying the involvement of CALM in other important hematopoietic processes. Several such experiments are currently underway in our laboratory.

Acknowledgments

We would like to thank Dr. Issay Kitabayashi (National Cancer Center Research Institute, Tokyo, Japan) for stimulating and useful discussions, advice, and helpful comments on our results.

Author Contributions

Conceived and designed the experiments: TW MS HT K. Tanabe. Performed the experiments: MS HT AT K. Tanabe NO SR MF K. Takei TA IM TW. Analyzed the data: TW MS HT K. Tanabe. Contributed reagents/materials/analysis tools: SK IM YK. Wrote the paper: MS TW HT YK.

References

1. Kirchhausen T (2000) Clathrin. Annu Rev Biochem 69: 699–727.
2. Kirchhausen T, Harrison SC (1981) Protein organization in clathrin trimers. Cell 23: 755–761.
3. Marsh M, McMahon HT (1999) The structural era of endocytosis. Science 285: 215–220.
4. Schmid EM, McMaho HT (2007) Integrating molecular and network biology to decode endocytosis. Nature 448: 883–888.
5. Ungewickell E, Branton D (1981) Assembly units of clathrin coats. Nature 289: 420–422.
6. Motley A, Bright NA, Seaman MN, Robinson MS (2003) Clathrin-mediated endocytosis in AP-2-depleted cell. J Cell Biol 162: 909–918.
7. Robinson MS (2004) Adaptable adaptors for coated vesicles. Trends Cell Biol 14: 167–174.
8. Ahle S, Ungewickell E (1986) Purification and properties of a new clathrin assembly protein. EMBO J 5: 3143–3149.
9. Ford MG, Pearse BM, Higgins MK, Vallis Y, Owen DJ, et al. (2001) Simultaneous binding of PtdIns(4,5)P2 and clathrin by AP180 in the nucleation of clathrin lattices on membranes. Science 291: 1051–1055.
10. Gillooly DJ, Stenmark H (2001) A lipid oils the endocytosis machine. Science 291: 993–994.
11. Meyerholz A, Hinrichsen L, Groos S, Esk PC, Brandes G, et al. (2005) Effect of clathrin assembly lymphoid myeloid leukemia protein depletion on clathrin coat formation. Traffic 6: 1225–1234.
12. Ford MG, Mills IG, B. Peter BJ, Vallis Y, Praefcke GJ, et al. (2002) Curvature of clathrin-coated pits driven by epsin. Nature 419: 361–366.
13. Hom RA, Vora M, Regner M, Subach OM, Verkhusha VV, et al. (2007) pH-dependent binding of the Epsin ENTH domain and the AP180 ANTH domain to PI(4,5)P2-containing bilayers. J Mol Biol 373: 412–423.
14. Legendre-Guillemin V, Wasiak S, Hussain NK, Angers A, McPherson PS (2004) ENTH/ANTH proteins and clathrin-mediated membrane budding. J Cell Sci 117: 9–18.
15. Tebar F, Bohlander SK, Sorkin A (1999) Calthrin assembly lymphoid myeloid leukemia (CALM) protein: localization in endocytic-coated pits, interactions with clathrin, and the impact of overexpression on clathrin-mediated traffic. Mol Biol Cell 10: 2687–2702.
16. Dreyling MH, Martinez-Climent JA, Zheng M, Mao J, Rowley JD, et al. (1996) The t(10;11)(p13;q14) in the U937 cell line results in the fusion of the AF10 gene and CALM, encoding a new member of the AP-3 clathrin assembly protein family. Proc Natl Acad Sci *USA* 93: 4804–4809.
17. Caudell D, Aplan PD (2008) The role of CALM-AF10 gene fusion in acute leukemia. Leukemia 22: 678–685.
18. Deshpande AJ, Cusan M, Rawat VP, Reuter H, Krause A, et al. (2006) Acute myeloid leukemia is propagated by a leukemic stem cell with lymphoid characteristics in a mouse model of CALM/AF10-positive leukemia. Cancer Cell 10: 363–374.
19. Klebig ML, Wall MD, Potter MD, Rowe EL, Carpenter DA, et al. (2003) Mutations in the clathrin-assembly gene Picalm are responsible for the hematopoietic and iron metabolism abnormalities in fit1 mice. Proc Natl Acad Sci USA 100: 8360–8365.